Pergamon

www.elsevier.com/locate/neuroscience

PII: S0306-4522(01)00033-1

Neuroscience Vol. 103, No. 3, pp. 777–797, 2001

0306-4522/01 $20.00+0.00

GENE EXPRESSION AND PROTEIN DISTRIBUTION OF THE OREXIN-1 RECEPTOR IN THE RAT BRAIN AND SPINAL CORD

G. J. HERVIEU,* J. E. CLUDERAY, D. C. HARRISON, J. C. ROBERTS and R. A. LESLIE

Department of Neuroscience, SmithKline Beecham Pharmaceuticals, Third Avenue, Harlow, Essex CM19 5AW, UK

Abstract—Orexins-A and -B are neuropeptides derived from a single precursor prepro-orexin. The mature peptides are mainly expressed in the lateral hypothalamic and perifornical areas. The orexins have been implicated in the control of arousal and appear to be important messengers in the regulation of food intake. Two receptors for orexins have been characterised so far: orexin-1 and -2 receptors. To gain a further understanding of the biology of orexins, we studied the distribution of the orexin-1 receptor messenger RNA and protein in the rat nervous system. We first assessed the expression profile of the orexin-1 receptor gene (*ox-r1*) in different regions by using quantitative reverse transcription followed by polymerase chain reaction. Using immunohistochemical techniques, we investigated the distribution of orexin-1 receptor protein in the rat brain using a rabbit affinity-purified polyclonal antiserum raised against an N-terminal peptide. The orexin-1 receptor was widely and strongly expressed in the brain. Thus, immunosignals were observed in the cerebral cortex, basal ganglia, hippocampal formation, and various other subcortical nuclei in the hypothalamus, thalamus, midbrain and reticular formation. In particular, robust immunosignals were present in many hypothalamic and thalamic nuclei, as well as in the locus coeruleus. The distribution of the receptor protein was generally in agreement with the distribution of the receptor messenger RNA in the brain as reported previously by others and confirmed in the present study. In addition, we present *in situ* hybridisation and immunohistochemical data showing the presence of orexin-1 receptor messenger RNA and protein in the spinal cord and the dorsal root ganglia. Finally, due to the shared anatomical and functional similarities between orexins and melanin-concentrating hormone, we present a comparison between the neuroanatomical distribution of the orexin-1 receptor and melanin-concentrating hormone receptor protein-like immunoreactivities in the rat central nervous system, and discuss some functional implications.

In conclusion, our neuroanatomical data are consistent with the biological effects of orexins on food intake and regulation of arousal. In addition, the data suggest other physiological roles for orexins mediated through the orexin-1 receptor. © 2001 IBRO. Published by Elsevier Science Ltd. All rights reserved.

Key words: neuropeptide, antiserum, rat, immunohistochemistry, *in situ* hybridisation.

The orexins[38] and hypocretins[8] represent a recently characterised family of hypothalamic neuropeptides. Proteolytic maturation of the 130-amino-acid-long prepro-orexin protein allows the release of orexin-A and orexin-B (33 and 28 amino acids long, respectively; 46% sequence identity). The prepro-orexin gene is specifically expressed in the lateral hypothalamus (LHA)[38] and orexin-containing processes are found widely throughout the CNS.[6,7,37,52] The LHA, traditionally viewed as a phylogenetic continuation of the reticular formation, governs many functions, such as feeding, blood pressure, neuroendocrine axis, thermoregulation, sleep–waking cycle, emotion, sensorimotor integration and reward processes. This reflects their extensive projections throughout the nervous system, including monosynaptic projections to several regions of the cerebral cortex, limbic system and brainstem, and innervation of the major catecholaminergic and serotonergic systems (e.g. raphe nuclei and locus coeruleus).[1] Of these diverse roles of the LHA, feeding behaviour regulation is a major one: the so-called lateral hypothalamic feeding syndrome, due to lesions of the LHA, causes death because of aphagia and loss of weight. The concept developed is that of a dual-control centre of feeding, with the LHA being the feeding centre and the ventromedial hypothalamic nuclei the satiety centre. The hypothesis has suffered from a number of caveats, but the recent discovery that the LHA contains at least two major orexigenic peptides, melanin-concentrating hormone (MCH)[39] and the orexins,[40] is strongly supportive of it. Energy metabolism is also thought to be critically controlled by the LHA, as it contains a population of neurones which are sensitive to glucose levels and are activated by hypoglycaemia. The identity of these cells has remained elusive, probably because the LHA is not as topologically organised as other major nuclei of the

*Corresponding author. Tel.: +44-1279-622931; fax: +44-1279-622230.

E-mail address: guillaume_hervieu-1@sbphrd.com (G. J. Hervieu).

Abbreviations: BSA, bovine serum albumin; EDTA, ethylenediaminetetra-acetate; GAPDH, glyceraldehyde-3-phosphate dehydrogenase; HEK, human embryonic kidney; LHA, lateral hypothalamic area; MCH, melanin-concentrating hormone; *ox-r1*, orexin-1 receptor gene/cDNA; *ox-r2*, orexin-2 receptor gene/cDNA; OX-R1, orexin-1 receptor protein; OX-R2, orexin-2 receptor protein; PBS, phosphate-buffered saline; PCR, polymerase chain reaction; RT, reverse transcription; SLC-1, generic name of the MCH receptor.

Abbreviations used in the figures

ACA	anterior cingulate area
AD	anterodorsal thalamic nucleus
AHN	anterior hypothalamic nucleus
Al(d) (p) (v)	agranular insular area, (dorsal) (posterior) (ventral) parts
AMd	anteromedial nucleus thalamus (dorsal part)
AON	anterior olfactory nucleus
APN	anterior pretectal nucleus
AQ	cerebral aqueduct
Arc	arcuate nucleus
AUD(p) (v) (d)	auditory area (primary) (ventral) (dorsal)
AV	anteroventral thalamic nucleus
BMA(a)	basomedial nucleus of the amygdala (anterior part)
BST	bed nuclei of the stria terminalis
C	colliculus
C(M) (L)	(mediocentral) (laterocentral) thalamic nucleus
CA(1) (2) (3)	Ammon's horn fields (1) (2) (3)
CA(so) (sp)	Ammon's horn field, stratum (oriens) (pyramidal)
cb	cerebellum
cc	corpus callosum
CL	central lateral nucleus
CLA	claustrum
CM	central medial thalamic nucleus
COA	cortical nucleus of the amygdala
CP	caudate–putamen
cpd	cerebral peduncle
cst	corticospinal tract
DCO	dorsal cochlear nucleus
DG(cr) (sg)	dentate gyrus, (crest) (granule cell) layers
DMH	dorsomedial hypothalamic nucleus
DR	dorsal nucleus raphe
DRG	dorsal root ganglion
DTN	dorsal tegmental nucleus
ECT	ectorhinal area
ECU	external cuneate nucleus
ENT(l)	entorhinal area (lateral)
EPd	endopiriform nucleus, dorsal part
EPN	entopeduncular nucleus
EW	Edinger–Westphal nucleus
fa	anterior forceps of the corpus callosum
fx	fornix
GP(m) (l)	globus pallidus (medial) (lateral)
GRN	gigantocellular reticular nucleus
GU	gustatory area
gVIIn	genu of the facial nerve
hi	hippocampus
IC	inferior colliculus
III	principal oculomotor nucleus
ILA	infralimbic area
INC	interstitial nucleus of Cajal
Int(A) (P)	interpositus cerebellar nucleus, (anterior) (posterior) subdivisions
IO(da) (ma) (pr)	inferior olivary complex, (dorsal accessory) (medial accessory) (principal) parts
IPN	interpeduncular nucleus central subnucleus
isl	islands of Calleja
LC	locus coeruleus
LD	lateral dorsal nucleus
LG	lateral geniculate complex
LH	lateral habenula
LM	lateral mammillary hypothalamic nucleus
LS(d) (i)	lateral septum, (dorsal) (intermediate) segments
MA	magnocellular preoptic nucleus
MARN	magnocellular reticular nucleus
MDl	mediodorsal thalamus, lateral part
MDRNv	medullary reticular nucleus, ventral part
MEA	medial amygdaloid nucleus
MedDL	medial cerebellar nucleus, dorsal protuberance
MEPO	median preoptic nucleus
MG(v)	medial geniculate complex (ventral element)
MH	medial habenula
ml	medial lemniscus (Reil)
mlf	medial longitudinal fasciculus
MM	medial mammillary nucleus
MO(p) (s)	(primary) (secondary) motor area
MPT	medial pretectal area
MRN	mesencephalic reticular nucleus
MS	medial septal nucleus
MV	medial vestibular nucleus
NB	nucleus brachium
ND	nucleus of Darkschewitsch
NDB	nucleus of the diagonal band
NLL	nucleus of the lateral lemniscus
NTB	nucleus of the trapezoid body
opt	optic tract
OT	olfactory tubercle
PA	posterior nucleus of the amygdala
PAG	periaqueductal gray matter
PARN	parvicellular reticular nucleus
PCG	pontine central gray
PCN	paracentral thalamic nucleus
PERI	perirhinal area
PF	parafascicular thalamic nucleus
PG	pontine gray
PGRNl	paragigantocellular reticular nucleus, lateral part
PH	posterior hypothalamic nucleus
PIR	piriform cortex
PL	prelimbic area
PM(d)	posterior mammillary nucleus (dorsal)
POR	periolivary complex
PPN	pedunculopontine nucleus
PRN(c) (r)	pontine reticular nucleus, (caudal) (rostral) parts
PSV	principal sensory trigeminal nerve
PT	parataenial thalamic nucleus
PTLp	posterior–parietal region association area
PV(p)	periventricular hypothalamic nucleus, (posterior) part
PVH(dp) (mpv) (pml) (pmd) (pv)	paraventricular hypothalamic nucleus (dorsal parvicellular) (medial parvicellular) (posterior magnocellular, lateral zone) (medial parvicellular, dorsal zone) (periventricular zone)
PVT	paraventricular thalamic nucleus
py	pyramidal tract (Vieussens)
RN	red nucleus
RSP(d) (v)	retrosplenial cortex, (dorsal) (ventral) parts
RT	reticular thalamic nucleus
SC(sg) (ig) (dg) (zo)	superior colliculus, (superficial gray) (intermediate gray) (deep gray) (zonal) layers
SCH	suprachiasmatic hypothalamic nucleus
scp	superior cerebellar peduncle
SG	supragenual nucleus
SGN	suprageniculate nucleus
SI	substantia innominata
SLC	subcoeruleus nucleus
sm	stria medullaris
SNp(c) (r)	substantia nigra pars (compacta) (reticulata)
SO	supraoptic nucleus
so	stratum oriens
SOC(l)	superior olivary complex, (lateral) part
sp, SP	pyramidal layer
SPIV	spinal vestibular nucleus
sptV	spinal tract of the trigeminal nerve
SPV(o) (I) (C)	nucleus of the spinal tract trigeminal nerve, (oral) (interpositus) (caudal) part
SS(p) (s)	(primary) (secondary) somatosensory area
STN	subthalamic nucleus
SUB(d)	subiculum (dorsal part)
TEv	ventral temporal association area
TM(v)	tuberomammillary hypothalamic nucleus (ventral)
TRN	tegmental reticular nucleus
tsp	tectospinal pathway
TT(d)	tania tecta (dorsal)
3v	third ventricle
4v	fourth ventricle

V	motor nucleus of the trigeminal nerve
VAL	ventral anterior–lateral thalamic complex
VCO	ventral cochlear nucleus
VI	abducens nucleus
VII	facial nucleus
VIP	velum interpositum
VIS(al) (am) (li) (ll) (p) (pl) (pm)	(anterolateral) (anteromedial) (intermediolateral) (laterolateral) (primary) (posterolateral) (posteriomedial) visual area
VISC	visceral area
VMH(c) (dm) (vl)	ventromedial hypothalamic nucleus, (central) (dorsomedial) (ventrolateral) parts
VP(L) (M)	ventral postero(lateral) (medial) thalamic nucleus
VTA	ventral tegmental area
ZI	zona incerta

hypothalamus. In addition, the medial forebrain bundle, the most prominent brain fibre network bundle, passes through the LHA; this has added complexity to the design of experiments to study the LHA that would not damage the medial forebrain bundle itself. It may be that some orexin neurones are the anatomical substrate of the hypothalamic glucostat (see Ref. 29) rather than the formerly suspected MCH neurones.[12] The fact that insulin-induced hypoglycaemia greatly increases the level of prepro-orexin precursor protein (see Ref. 41) also suggests that this may be the case. Since, like most peptides, the orexins can be described as "gut-brain" peptides,[23] they may act as integration signals between the CNS and the enteric nervous system. Another major role recently discovered for orexins concerns their role in sleep and arousal mechanisms[5,13,26,33,38,48,49] (for reviews, see Refs 34, 44 and 50).

The actions of orexins/hypocretins are mediated via two G-protein-coupled receptors named the orexin-1 (OX-R1) and orexin-2 (OX-R2) receptors.[40] Some confusion has arisen in the literature because of reports that orexins and hypocretins are alternative names for the same peptides acting on the same receptors. The hypocretins were also described as hypothalamic neuropeptides, but their biological role was not described. Alignment of their nucleotide sequences shows that hypocretins-1 and -2 have sequence in common with orexins-A and -B, respectively, but additional amino acids were deduced to be present in both hypocretins: six extra amino acids in hypocretin-1 (five at the N-terminus and one at the C-terminus), and one extra in hypocretin-2 (at the C-terminus). In contrast to the hypocretins, the orexins were isolated and identified directly from rat brain and bovine hypothalamic extracts. It was also recently reported that hypocretins are at least 1000 times weaker at OX-R1 and OX-R2 than the orexins.[45,46] Few data are available on OX-R1 and OX-R2 localisation within the CNS. To date, only one report has explored the distribution of the mRNA encoding OX-R1 and OX-R2 in the rat brain by mRNA *in situ* hybridisation.[51] Orexin-A binds equally to both subtypes, while orexin-B has a preferential affinity for OX-R2.[40] In the absence of highly selective ligands to distinguish the receptor subtypes and given the importance of the biological roles of orexins, receptor antibodies are needed to discriminate between them. In this study, we investigated the gene expression regional distribution of the *ox-r1* gene in the rat CNS and the immunohistochemical pattern of OX-R1-like immunoreactivity in the rat CNS using an affinity-purified antiserum raised against a N-terminal peptide specific for OX-R1.

Part of this work has been presented in abstract form.[20]

EXPERIMENTAL PROCEDURES

Animals

Adult male Sprague–Dawley rats (200–250 g; Charles River, UK) were kept in a fixed 12-h light–dark cycle with food and water provided *ad libitum*. All animal experiments were carried out in accordance with the UK Animals (Scientific Procedures) Act (86609EEC) and all efforts were made to minimise the number of animals used and their suffering.

Peptides

All peptides were synthesised using solid-phase methodology on a model 432A Applied Biosystem Synthethiser. Peptide purity was estimated by chromatography as being greater than 95%.

Chemicals

All chemicals were purchased from Merck (UK) unless otherwise stated. The bovine serum albumin (BSA) used in all experiments was of a high-quality crystalline grade (Fraction V, A-8022, Sigma, UK). The peripherin antiserum was purchased from Chemicon Ltd (mouse monoclonal; MAB1527).

Cell culture

Human embryonic kidney (HEK) 293 cell lines were stably transfected with a human *ox-r1* cDNA subcloned using the pCDN vector (Invitrogen, Groningen, The Netherlands). All cell culture reagents were purchased from Life Technologies (Paisley, UK) and plasticware from Costar (High Wycombe, UK). Wild-type and OXR-1-transfected HEK293 cells were cultured in minimal essential medium containing Earle's Salts, L-glutamine, 10% fetal bovine serum, 1% minimal essential medium non-essential amino acids and 50 mg/ml Geneticin solution in humidified air containing 5% CO_2 at 37°C.

Quantitative reverse transcription–polymerase chain reaction analysis

For mRNA localisation studies, male Sprague–Dawley rats (300–350 g) were killed by CO_2 asphyxia followed by cervical dislocation. Sixteen brain regions, spinal cord and dorsal root ganglia were dissected. Each tissue was pooled from between six and 16 rats depending on the size of the individual tissue samples obtained. Total RNA was extracted from the tissue using TRIzol reagent (Life Technologies) according to the manufacturer's suggested protocol, with the addition of an extra chloroform extraction step and phase separation, and an extra wash of the isolated RNA in 70% ethanol. The RNA was resuspended in autoclaved, ultrapure water and the concentration calculated by A_{260} measurement. RNA quality was assessed by electrophoresis on a 1% agarose gel.

First strand cDNA synthesis was carried out by oligo(dT) priming from 1 μg of each RNA sample [0.01 M dithiothreitol, 0.5 mM each dNTP, 0.5 μg oligo(dT) primer, 40 U RNAaseOUT ribonuclease inhibitor (Life Technologies), 200 U Superscript II reverse transcriptase (Life Technologies)]. Triplicate reverse transcription (RT) reactions were performed along with an additional reaction in which the reverse transcriptase was omitted to allow for assessment of genomic DNA contamination of the RNA. The resulting cDNA products were divided into 20 aliquots for parallel Taqman polymerase chain reactions (PCRs) using

different primer and probe sets for quantification of multiple cDNA sequences.

Quantitative RT–PCR was carried out using an ABI 7700 sequence detector (Perkin Elmer, CA, USA) on the cDNA samples [2.5 mM $MgCl_2$, 0.2 mM dATP, dCTP, dGTP and dUTP, 0.1 μM each primer, 0.05 M Taqman probe, 0.01 U AmpErase uracil-*N*-glycosylase (Perkin Elmer), 0.0125 U Amplitaq Gold DNA polymerase (Perkin Elmer); 50°C for 2 min, 95°C for 10 min, followed by 40 cycles of 95°C for 15 s, 60°C for 1 min]. Additional reactions were performed on each 96-well plate using known dilutions of rat genomic DNA or plasmid DNA containing an *ox-r1* insert as a PCR template to allow construction of a standard curve relating threshold cycle to template copy number.

Taqman primer and probe sets for *ox-r1* and for the housekeeping gene glyceraldehyde-3-phosphate dehydrogenase (GAPDH) were designed using Primer Express software (Perkin Elmer). Parallel Taqman PCRs were run on each sample using the GAPDH primers and probe to control for RNA integrity.

Primer and probe sequences (forward primer, reverse primer and Taqman probe, respectively) were as follows: 5′-GGC-TGGTGTACGCCAACAG, 5′-TTGAACTGCTCCCGAAATTTG and 5′-CGGCCAACCCTATCATCTACAACTTCCT (for *ox-r1*); 5′-GAACATCATCCCTGCATCCA, 5′-CCAGTGAGCTTCCCG-TTCA and 5′-CTTGCCCACAGCCTTGGCAGC (for GAPDH).

Copy numbers obtained for *ox-r1* were normalised to those for GAPDH and the resulting values expressed as arbitrary units (normalised to the whole brain value; $y = 1$). The absolute values given to the expression levels are therefore arbitrary, and it is the relative expression of this transcript in different brain areas that is shown. For more details, refer to Ref. 14.

In situ hybridisation

Full details of the *in situ* hybridisation protocol have been reported elsewhere.[16] Briefly, fresh-frozen rat brain sections (cut coronally or sagittally with a thickness of 20 μm) were hybridised overnight with ^{35}S-radiolabelled oligoprobes designed from the rat *ox-r1* cDNA sequence.[38] Washed and dehydrated sections were exposed to Kodak Biomax film for up to five days. Various oligonucleotides with non-overlapping sequences were optimally designed using the Primer select software within the Lasergene package (no significant hairpin formation or primer dimerisation potential under the hybridisation conditions used). Oligonucleotides were used independently (sense sequences: 5′-GGC GGAACC ACC ACA TGA GGA CAG T-3′ starting at position 215 as compared to the start codon of the *ox-r1* cDNA gene sequence; 5′-CTT CTT CTT TGT CAC CTA CCT GGC CCC GCT-3′ starting at position 654 as compared to the start codon of the *ox-r1* cDNA sequence; 5′-CAT TCT CCT GCT GCC TGC CTG GTC TGG GTC-3′ starting at position 1115 as compared to the start codon of the *ox-r1* gene sequence) and provided similar patterns of distribution. Because of the sequence identity between *ox-r1* and *ox-r2* cDNA, an oligonucleotide was designed to recognise only the *ox-r2* sequence (sense sequence: 5′-TTGGCT GCT GGG AGT GTG CTT ATG CTG GTG-3′ starting at position 1275 as compared to the start codon of the *ox-r2* sequence as given in Ref. 38). Sequences were checked for uniqueness against the BLAST program (Advanced search; GenEMBL complete). Control included the use of the sense sequence oligoprobe and the use on an excess (100 times) of unlabelled antisense oligoprobes mixed with radiolabelled antisense oligoprobes.

Western blot analysis

Extracts from wild-type or *ox-r1* cDNA-transfected HEK293 cells were prepared by shearing cell pellets in lysis buffer [20 mM Tris, 5 mM EDTA, 150 mM NaCl, 0.4% Triton X-100 (Sigma, UK), 0.4% Nonidet P-40 (Sigma, UK), pH 7.4] followed by centrifugation at 6000 r.p.m. Supernatant was removed and protein concentration was measured by Bradford assay (Biorad, UK).

For western blot analysis, cell extracts were resolved by sodium dodecyl sulphate–polyacrylamide gel electrophoresis (4–20%), loading 10 μg protein per lane, and transferred onto nitrocellulose (Schleicher & Schuell, Germany). The membrane was blocked with 10% low fat milk (Marvel, UK), 0.5% Tween 20 in phosphate-buffered saline (PBS) for 1 h and revealed using an immunoglobulin-enriched fraction of the crude OX-R1 antiserum at 1:2000, followed by incubation with peroxidase-conjugated secondary antibody (Amersham, UK). Bound antibody was detected using the Enhanced ChemiLuminescence ECL kit (Amersham, UK).

Immunohistochemistry

Rabbit polyclonal antisera were raised against a peptide derived from the human and rat OX-R1 sequence.[40] The 16-amino-acid-long peptide (H-*EPS ATP GAQ PGV* PTS S-OH) is located in the N-terminal extracellular tail, amino acids 2–17 (rat and human). It is fully identical to the rat sequence. Amino acid changes in the human sequence are indicated in bold: H-EPS ATP GAQ **M**GV P**PG** S-OH. The synthetic peptide was covalently NH_2-coupled to the carrier keyhole limpet haemocyanin using the glutaraldehyde method. The crude antiserum was affinity purified using the immunogenic peptide linked to BSA and bound to a nitrocellulose membrane or using an affinity chromatography column with a Sulfolink matrix covalantly linked to the N-terminal cysteine-extended immunogenic peptide.

Immunohistochemistry and immunocytochemistry were carried out with an avidin–biotin–peroxidase complex (ABC kit, Vector Laboratories, UK) reporter system as described previously[18] or by immunofluorescence.[17] Briefly, adult male Sprague–Dawley rats ($n = 5$) were anaesthetised with pentobarbital prior to transcardiac perfusion with 4% paraformaldehyde in PBS. Cryostat-cut coronal sections (35 μm) were incubated in PBS containing 20% methanol and 1.5% hydrogen peroxide for 30 min in order to quench the endogenous pseudo-peroxidase activity, washed in PBS, and incubated in a blocking solution (3% normal goat serum, 2 g/l BSA, 0.1% Triton X-100 in PBS). Sections were then incubated with the primary antiserum (dilution 1:10) for 48 h at 4°C with gentle agitation. In co-localisation experiments, the peripherin monoclonal antiserum was used at 1:200. After primary incubation, sections were given three 10-min washes in 0.3% Triton X-100 in PBS. Sections were then processed for immunostaining using an avidin–biotin–peroxidase complex (ABC kit, Vector Laboratories) amplification system following the manufacturer's recommendations unless indicated. Immunosignals were developed with 3,3′-diaminobenzidine substrate (Vector Laboratories) for 5–10 min before the reaction was stopped in distilled water. Sections were mounted onto Superfrost polished slides (BDH, UK), allowed to air dry, then coverslipped with DPX mountant. Alternatively, and where indicated, immunochemical fluorescence was carried out as described previously[17] using streptavidin-conjugated fluorophores (Cy2, Cy5; Jackson Laboratories, USA).

Immunocytochemistry

Wild-type or OX-R1-transfected HEK293 cells were grown on LabTek slides (Life Technologies) and fixed for 15 min in 4% w/v paraformaldehyde in 0.1 M PBS. The fluorescence immunocytochemical procedure was similar to that already described for immunohistochemistry.

Control experiments included the omission of the primary antiserum, the use of rabbit pre-immune serum and pre-absorbing the antiserum with the immunogenic peptide. Pre-absorption controls were done with 10 μM of the immunogenic peptide (incubated overnight with the antiserum prior to the incubation on sections). Specificity of the antisera was investigated on OX-R1 HEK293-transfected cells versus wild-type cells, with or without pre-absorption, with or without primary antisera in a fluorescence procedure.

Histological analysis

Brain regions and nuclei were identified using the rat brain

atlases of Paxinos and Watson[36] for sagittal sections and Swanson[47] for coronal sections. The nomenclature adopted is mainly that from Swanson.[47]

Differences in plane of section for sagittal and coronal dimensions as compared to atlases were corrected by mapping immunostained regions onto appropriate parts of a series of adjacent sections, as proposed by Swanson.[47]

The scoring system used relied on the evaluation of immunosignal intensity (brown deposit of oxidised 3,3′-diaminobenzidine) as judged by two independent investigators with $n = 5$ rats. The relative density of labelling was classified as absent (−), sparse (+), moderate (++), extensive (+++) or very extensive (++++).

Image acquisition and processing

In situ hybridisation data were captured with a Pulnix TM-765 black and white camera coupled to a Tamron SP system. Peroxidase immunohistochemical data were captured with a JVC 3CCD KY-F55B colour video camera or a Leica DC 200 digital camera. Fluorescence immunohistochemical and immunocytochemical data were analysed with a Leica TCS confocal DM RB microscope. Confocal images were either taken as a 0.8-μm-thick single plane or as a stack of several planes (and thereafter reconstructed in three dimensions through a Projection function). Each single plane was averaged four times.

Image acquisition for *in situ* hybridisation and peroxidase data was carried out with Image ProPlus software (Media Cybernetics, USA). Images were taken with the highest level of contrast and brightness. Images were imported into PaintShop Pro Version 5.0 (Jasc Software, USA). Image modification involved the transformation of colour images into black and white images using a grey scale function, and adjusting the levels of brightness and contrast. The images were sharpened through a "sharpen" function.

RESULTS

Taqman reverse transciption–polymerase chain reaction analysis of orexin-1 receptor mRNA expression in rat nervous system

The primary data generated by Taqman RT–PCR consist of a threshold cycle value, indicating the PCR cycle at which the PCR product is detectable above an arbitrary threshold. The system was calibrated using known numbers of copies of genomic DNA. When the threshold cycle generated by these standards was plotted against the genomic DNA copy number on a logarithmic scale, the data points lay on a straight line (not shown). With threshold cycle values resulting from the cDNA samples from various tissues, a copy number was read from this calibration curve. The mRNA encoding OX-R1 was widely distributed throughout the CNS (Fig. 1A). mRNA was detected in all regions tested with the exception of the cerebellum. Highest levels of expression were observed in the hypothalamus, substantia nigra and thalamus. Data have been normalised to GAPDH levels to control for variations in RNA quality and loading. Only slight variations in GAPDH mRNA expression were observed between the tissues that were included in the study (data not shown).

Immunochemical studies

Specificity of the antiserum as determined by immunocytochemistry. Specific immunocytochemical signals (Fig. 1C), largely confined to the plasma membrane, were generated with OX-R1-transfected HEK293 cells incubated with the affinity-purified OX-R1 antiserum, as opposed to the control condition using the wild-type HEK293 cells incubated with the affinity-purified OX-R1 antiserum (Fig. 1B).

Specificity of the antisera as determined by immunohistochemistry using rat brain tissue sections. A distinctive immunostaining pattern was obtained after incubation of brain sections in the affinity-purified antiserum (Fig. 1D, F). In control experiments using the antiserum pre-absorbed with the immunogenic peptide, the immunosignal intensity was diminished (Fig. 1E, G).

Specificity of the oligoprobes as determined by in situ hybridisation on rat brain tissue sections. Specific autoradiographic signals were obtained, with discrete anatomical localisation, using the radiolabelled antisense oligoprobes (Fig. 1H). Specific signals were encountered in the cerebral cortex, the hippocampus (pyramidal layers of the CA fields and the granular layer of the dentate gyrus) and the hypothalamic medial tuberal nucleus. A specific and strong signal was obtained in the locus coeruleus. In a control experiment, the use of the sense oligoprobe produced no substantial tissue labelling (Fig. 1I). The signal obtained in the cerebellum was not specific as it could not be abolished by mixing the radioactive probes with an excess of unlabelled probes (not shown).

Histological localisation studies in the brain and spinal cord

The distribution of OX-R1-like immunoreactivity in the brain and spinal cord is shown in Table 1.

Forebrain: telencephalon. Isocortex. Heavy protein labelling was observed in the cerebral cortex. Many isocortical subregions were immunopositive, amongst them the primary and secondary motor areas (Fig. 2A), the claustrum (Fig. 2B), the primary and secondary somatosensory areas (Fig. 2B, D), gustatory area (Fig. 2B), anterior cingulate area (Fig. 2B), visceral area (Fig. 2D), the dorsal, ventral and posterior parts of the agranular insular area (Fig. 2A, B, D), retrosplenial cortex (Fig. 2F), posterior–parietal region association area, dorsal auditory area, primary auditory area, ventral auditory area, primary auditory area, and anterolateral, primary, rostrolateral and anteromedial visual areas (Fig. 2E). Immunostaining was particularly concentrated in layers III and IV (Fig. 2F). Cells immunostained in these areas were labelled on their surface membranes (Fig. 4A, B). Most stained cells resembled principal neurones (Fig. 4B), but no processes were immunostained (either axons or dendritic trees).

Olfactory cortex. This region was heavily immunostained with the OX-R1 antiserum. Labelling was seen in the anterior olfactory nucleus (Fig. 2A) and olfactory tubercle (Fig. 2B). Dense signals were also observed in the dorsal part of the taenia tecta (Fig. 2C) and in the piriform cortex (Fig. 2B).

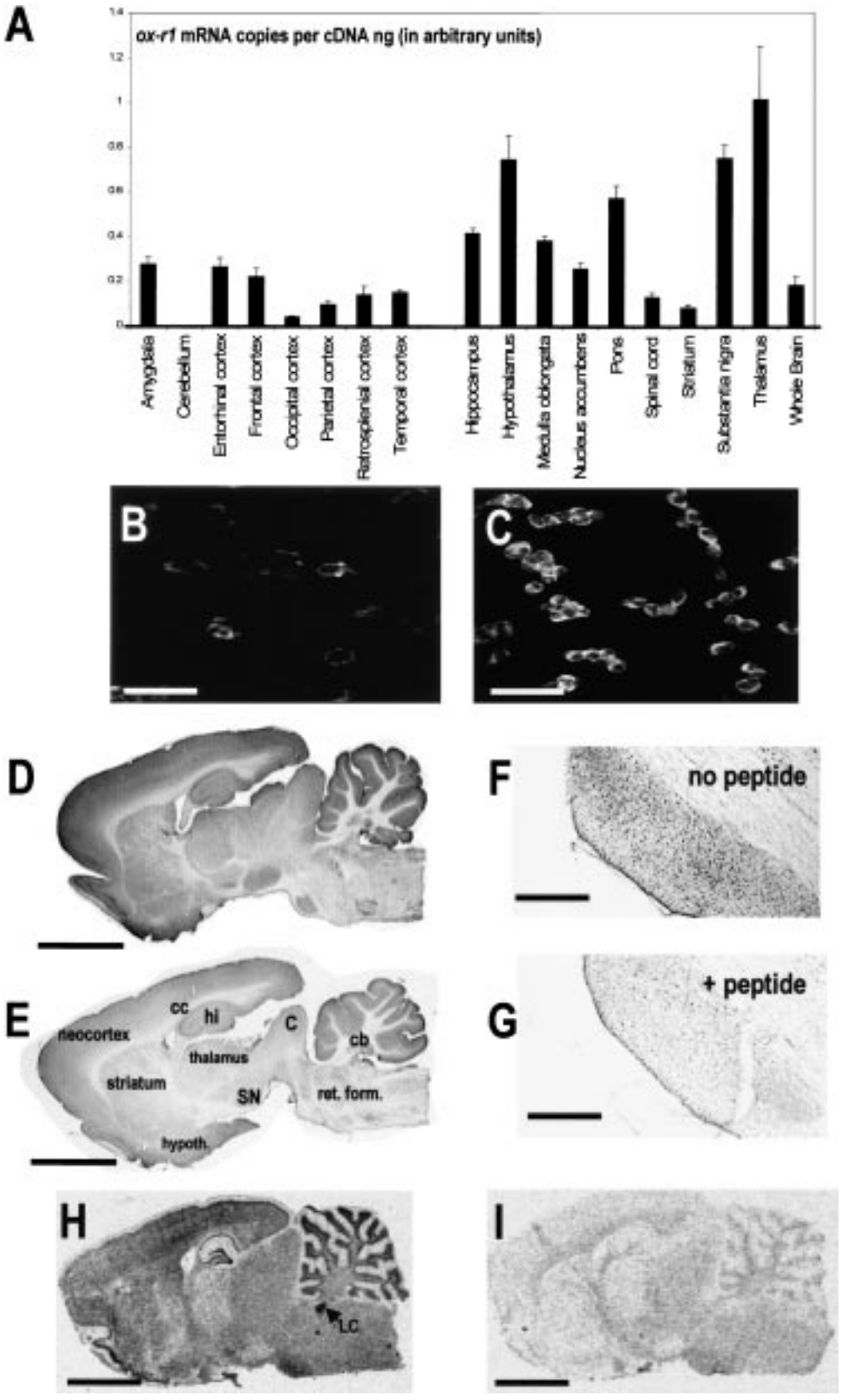
A
ox-r1 mRNA copies per cDNA ng (in arbitrary units)
1.4
1.2
1
0.8
0.6
0.4
0.2
0
Amygdala
Cerebellum
Entorhinal cortex
Frontal cortex
Occipital cortex
Parietal cortex
Retrosplenial cortex
Temporal cortex
Hippocampus
Hypothalamus
Medulla oblongata
Nucleus accumbens
Pons
Spinal cord
Striatum
Substantia nigra
Thalamus
Whole Brain
B
C
D
E
neocortex
cc
hi
C
cb
thalamus
striatum
SN
rot. form.
hypoth.
F
no peptide
G
+ peptide
H
LC
I

Fig. 1.

Hippocampal formation. The entorhinal area was strongly immunostained in its lateral part (Fig. 3C). In the hippocampus, all subfields of Ammon's horn were immunopositive, with CA2 and CA3 being more strongly labelled than CA1. Immunosignals were mainly located in the stratum pyramidale in Ammon's horn.The granule cell layer of the dentate gyrus was lightly stained (Fig. 4G). Interneurone-like cells were immunostained in the hilus (Fig. 4H).

Amygdala. The *ox-r1* gene was relatively highly expressed in amygdaloid regions. Protein signals were seen in the medial (anterior and anterodorsal part) and basomedial (anterior part) nuclei (Figs 2E, G and 3A).

Septal regions. The septum was immunolabelled in the medial septal nucleus, the nucleus of the diagonal band of Broca, the lateral septum (Fig. 2D) and the bed nucleus of the stria terminalis (Fig. 2E).

Corpus striatum. The caudate–putamen was labelled (Fig. 2D). The globus pallidus was stained in its lateral (Fig. 2E) and medial segments, where membrane-immunostained cells were seen (Fig. 5B, C). The substantia innominata and magnocellular preoptic nucleus were immunostained as well (Fig. 2C, E).

Forebrain: diencephalon. Epithalamus. In the epithalamus, signals were observed in the lateral habenula (Fig. 6A).

Thalamic nuclei. The thalamus contained high levels of OX-R1 signals. Progressing rostrally to caudally, on a ventral–caudal axis, OX-R1-like signals were detected in the reticular nucleus (Fig. 2F), paraventricular nucleus, parataenial nucleus, anterodorsal nucleus, anteroventral nucleus (Fig. 2G), lateral dorsal nucleus, ventral anterior–lateral complex (Fig. 2H), central medial, central lateral, paracentral, ventral posterior lateral and medial nuclei (Fig. 3A). The subthalamic nucleus and overlying zona incerta were also positive for OX-R1 immunosignals (Fig. 3C)

Metathalamus. Both the medial geniculate and lateral geniculate contained OX-R1-like immunolabelling (Fig. 3C).

Hypothalamus. OX-R1-like immunosignals were very dense in the hypothalamus. The suprachiasmatic nucleus was heavily immunostained (Figs 2E and 7C), as was the supraoptic nucleus (Figs 2E and 7A) and the arcuate nucleus (Fig. 7D). Strong signals were also obtained in the anterior nucleus (Fig. 3A), the ventromedial nucleus (Figs 3B and 7E, E′), the dorsomedial nucleus (Fig. 8F) and the lateral area (Figs 3B and 8G), as well as the overlying zona incerta (not shown). In the paraventricular nucleus, immunostaining was seen in the lateral zone of the posterior magnocellular region, and the dorsal parvicellular, medial parvicellular and dorsal zones of the medial parvicellular region (Fig. 8B). More rostrally, labelling was recorded in the posterior periventricular nucleus as well as the dorsal part of the posterior mammillary nucleus (Fig. 3D), the medial mammillary and tuberomammillary nuclei (Fig. 3E).

Midbrain and hindbrain: sensory. Visual areas. Signals were present within the superior colliculus, in the zonal and superficial gray layers, and were concentrated in the intermediate gray layers (Figs 3E and 6G). In the pretectal regions, immunostaining was present in the medial pretectal area (Fig. 6F).

Somatosensory areas. The principal sensory nucleus of the trigeminal was immunostained as well as the spinal nucleus of the trigeminal (Fig. 3H, I).

Auditory areas. The ventral cochlear nucleus was immunolabelled (Fig. 3F) as well as the dorsal cochlear nucleus (Fig. 8E). Strong immunostaining was found in the superior olivary complex, both in the lateral part of the superior olivary complex and periolivary complex (Figs 3F and 8F). The inferior colliculus was rich in OX-R1-like immunosignals (Fig. 6H) as well as the nucleus of the trapezoid body (Fig. 3H).

Vestibular areas. The medial vestibular nucleus was immunostained (Fig. 3H).

Visceral areas: motor. The trigeminal nucleus and the abduncens nucleus were immunostained (Fig. 3F, H). The Edinger–Westphal nucleus was also labelled with the OX-R1 antiserum (Fig. 3D). There was marked immunostaining in the facial nucleus (Fig. 3I).

Fig. 1. Regional rat nervous system expression profile of the *ox-r1* gene and specificity of the oligoprobes and antiserum used to detect gene and OX-R1 expression in the rat nervous system. (A) mRNA encoding OX-R1 is widely distributed throughout the rat nervous system, as investigated with a quantitative RT–PCR analysis. Message was detected in all regions tested with the exception of the cerebellum. Highest levels of expression were observed in the hypothalamus, substantia nigra and thalamus. *Ox-r1* gene expression was normalised to the expression of the housekeeping gene for GAPDH. Bars indicate the mean values derived from three independent RT–PCRs; error bars indicate S.E.M. (B, C) Wild-type HEK293 cells (B) and HEK293 OX-R1-transfected cells (C), grown on chamber microscopic slides, were incubated with affinity-purified anti-OX-R1 antiserum. Specific immunostaining can be seen in C, which proves the specificity of the antiserum for detecting OX-R1. (D–G) Rat brain sections were incubated with affinity-purified anti-OX-R1 antiserum followed by immunohistolabelling with horseradish peroxidase (D). Immunosignals were observed in the isocortex, basal ganglia (caudate–putamen), hippocampal formation, hypothalamus, thalamus and various midbrain areas (colliculus and reticular formation). When sections were incubated with antiserum pre-absorbed with the synthetic peptide, signal intensity was decreased (E). A close-up at the level of the pons is presented in F and G (control pre-adsorption condition). (H, I) Consecutive rat brain sections were hybridised with OX-R1 radiolabelled antisense oligonucleotides (H) or OX-R1 radiolabelled sense oligonucleotides (I). The use of sense oligoprobes (I) resulted in an absence of signal as compared with results obtained by using antisense oligoprobes (H). Note the very strong hybridisation signal obtained in the locus coeruleus. Also note that immunostained regions (D) were similar to the regions expressing mRNA (H). Scale bars = 50 μm (B, C), 500 μm (D, E, H, I), 300 μm (F, G).

Table 1. Distribution of orexin-1 receptor protein-like immunoreactivity in the rat brain

Region	Immunoreactivity
Telencephalon	
Olfactory system	
Olfactory nuclei	+++
Piriform cortex	+++
Taenia tecta	++
Neocortex	
Agranular insular cortex	+
Frontal cortex	++
Granular insular cortex	+
Parietal cortex	++
Metacortex	
Cingulate/retrosplenial cortex	++
Hippocampal formation	
CA1 region	+
CA2 region	++
CA3 region	+
Dentate gyrus	+++
Basal ganglia	
Caudate–putamen	+
Globus pallidus	++
Substantia nigra	++
Subthalamic nucleus	++
Amygdala	
Amygdaloid nuclei	++
Substantia innominata	++
Septal and basal magnocellular nuclei	
Bed nucleus of the stria terminalis	+++
Lateral septal nucleus, dorsal part	++
Medial septal nucleus	++
Nucleus of the horizontal limb of the diagonal band	++
Diencephalon	
Epithalamus	
Lateral habenula	++
Thalamus	
Anterodorsal thalamic nucleus	+++
Anteroventral thalamic nucleus	+
Centrolateral thalamic nucleus	+++
Centromedial thalamic nucleus	+
Medial habenular nucleus	++
Paracentral thalamic nucleus	++
Parataenial thalamic nucleus	++
Paraventricular thalamic nucleus	+
Reticular thalamic nucleus	+++
Ventral posterior thalamic nucleus	+++
Ventral anterior thalamic nucleus	+
Ventromedial thalamic nucleus	++
Zona incerta	+++
Metathalamus	
Lateral and medial geniculate nuclei	++
Subthalamus	
Subthalamic nucleus	++
Hypothalamus	++
Anterior hypothalamic area	+++
Arcuate hypothalamic nucleus	+++
Dorsomedial hypothalamic nucleus	+
Lateral hypothalamic area	++
Magnocellular preoptic nucleus	+
Medial mammillary nucleus	++
Paraventricular hypothalamic nucleus	+++
Periventricular hypothalamic nucleus	+++
Posterior hypothalamic area	++
Premammillary nucleus	++
Supraoptic nucleus	+++
Suprachiasmatic nucleus	+++
Ventromedial hypothalamic nucleus	+++
Mesencephalon	
Dorsal tegmental nucleus	+++
Inferior colliculus	+
Interpeduncular nuclei	++
Periaqueductal gray	++
Principal sensory trigeminal nucleus	++
Raphe nuclei	++
Red nucleus	+
Substantia nigra	++
Superior colliculus	+
Rhombencephalon	
Cochlear nucleus complex	+++
Facial nucleus	+++
Gigantocellular reticular nucleus	+
Locus coeruleus	++++
Olivary complex	+++
Pontine reticular nucleus	++
Spinal trigeminal nucleus	++
Vestibular nucleus (medial)	+
Cerebellum	
Cerebellar cortex	−
Deep cerebellar nuclei	++
Spinal cord and dorsal root ganglia	
Spinal cord (gray matter; dorsal and ventral horn)	+++
Dorsal root ganglia	+++

The relative density of labelling is classified as: −, absent; +, sparse; ++, moderate; +++, extensive; ++++, very extensive.

Visceral areas: extrapyramidal. Robust labelling was observed in the substantia nigra, both in the pars compacta (Figs 3C and 5D, F) and pars reticulata (Fig. 5E, F).

Pre- and post-cerebellar nuclei. The red nucleus contained immunolabelling (Fig. 5D), as well as the pontine central gray and the tegmental reticular nucleus (Fig. 3G).

Cerebellum. No immunolabelling was seen in the cerebellar cortex, but in the deep cerebellar nuclei instead (Fig. 8A). Also, the interpositus cerebellar nucleus was immunostained in both its anterior and posterior subdivisions, as well as the medial dorsolateral cerebellar nucleus (Fig. 8A–C).

Reticular core (including central gray and raphe). Central gray of the brain. Protein-like labelling was detected in the periaqueductal gray (Figs 3D, F and 6E). The dorsal tegmental nucleus was also immunostained, more strongly than the pontine central gray (Fig. 4H). The locus coeruleus was heavily positive for OX-R1 (Figs 3F and 8D). Immunoreactivity was also observed in the supragenual nucleus (Fig. 3H).

Interpeduncular nucleus. There was pronounced labelling of the interpeduncular nucleus (Fig. 3F).

Reticular formation. Weak staining was observed in

the caudal pontine reticular nucleus (Fig. 3F) and in the gigantocellular reticular nucleus (Fig. 3H).

Spinal cord (lumbar segment) and dorsal root ganglia: mRNA and protein distribution

There was strong mRNA and protein immunolabelling in the lumbar part of the spinal cord (Fig. 9A, B). All subdivisions of the gray matter (dorsal and ventral horn) were immunolabelled (ventromedial, dorsomedial, intermediolateral, central, ventrolateral, dorsolateral and retrodorsolateral). Immunostaining was observed in cell bodies of both the ventral (Fig. 9C) and dorsal (Fig. 9D) horn. *Ox-r1* gene products were also strongly expressed in the dorsal root ganglia, both at the mRNA and protein levels, in the lumbar part of the spinal cord (Fig. 9E, F). Strong immunostaining was seen in the dorsal root ganglia, with two types of cells being labelled based on morphometric characteristics (large and small cells; Fig. 9G). Co-localisation experiments with peripherin, a C-fibre marker, showed that some OX-R1-immunolabelled cells contained peripherin-like immunoreactivity (Fig. 9H).

DISCUSSION

In the present work, we have reported the distribution of OX-R1 protein in the rat CNS and its mRNA in the spinal cord and dorsal root ganglia by using quantitative RT–PCR, *in situ* hybridisation and immunohistochemistry. Specificity of the antiserum raised against an N-terminal peptide of the OX-R1 rat orthologue sequence[40] was demonstrated using OX-R1-transfected HEK293 cells. We could not detect a specific immunosignal in western blot experiments (after denaturing sodium dodecyl sulphate–polyacrylamide gel electrophoresis) using the antiserum and protein extracts of OX-R1-transfected cells. With immunocytochemistry, however, OX-R1-transfected cells were specifically labelled, mainly on their plasma membrane, as expected for the location of a G-protein-coupled receptor. These data may suggest that most of the antibodies present in the polyclonal serum recognised their peptide epitope in a conformational rather than in a continuous manner.

There was generally good agreement between the results of the present study and a previous study by Trivedi *et al*.[51] that used *in situ* hybridisation to examine tissue-specific *ox-r1* gene expression profiles within the rat brain. However, unlike Trivedi *et al*., we detected OX-R1 protein-like immunoreactivity in the olfactory tubercle, the medial septal nucleus, the nucleus of the diagonal band and, most importantly, in the lateral and paraventricular hypothamic nuclei. Given that both studies were semi-quantitative and not properly quantitative, and given also that the methodologies employed were different (mRNA vs protein), it is not possible to ascertain if these differences reflect genuine mechanisms at the level of post-transcriptional and traductional mechanisms, that ultimately determine the number of proteins generated by copy of OX-R1 mRNA. Clear immunostained cell soma were identified in the LHA and the paraventricular nucleus in our study, so that it is unlikely that the OX-R1 protein had been transported from another brain region where *ox-r1* gene transcription would have occurred. In the absence of electron microscopic studies, however, we cannot ascertain that the signals were not related to fibres coming closely into contact with the cell bodies.

Labelling was generally widespread throughout the brain, encompassing major cell groups in the forebrain, midbrain, hindbrain and spinal cord. Thus, our quantitative RT–PCR assay (Taqman analysis) detected the highest levels of *ox-r1* gene expression in the hypothalamus, substantia nigra and thalamus. High levels of *ox-r1* gene expression were also seen in the cerebral cortex, hippocampal formation, pons, medulla oblongata, spinal cord and dorsal root ganglia, while no labelling was detected in the cerebellar cortex. In addition, our *in situ* data confirmed the high expression of the *ox-r1* gene in the spinal cord as detected by Taqman analysis. As a control, we showed very high expression of the *ox-r1* gene in the locus coeruleus by *in situ* hybridisation, as reported.[51] All mRNA-positive regions were OX-R1-like immunoreactive as well. In the spinal cord and dorsal root ganglia, there was a precise overlap between the distributions of the OX-R1 mRNA and protein signals. Also, there was a good match between the receptor distribution described in the present study and the distribution of orexin-immunoreactive profiles within the rat brain as reported.[32,37,52]

The immunostaining described in the present study was restricted to the neuronal population, both in principal neurones (e.g. in the neocortex) and in interneurones (e.g. in the hippocampal hilus). Furthermore, signals were mainly confined to plasma membranes of cells, as would be expected for a G-protein-coupled receptor. Interestingly, the antiserum did not reveal any nerve fibre staining, but instead only soma staining.

Neuroanatomical distribution of orexin-1 receptor protein-like immunoreactivity and functional implications

The OX-R1 immunoreactivity found in various subnuclei of the hypothalamus is consistent with the energy and fluid balance regulatory properties of orexins.[15,25,40] Immunosignals in the paraventricular, arcuate and ventromedial nuclei and LHA/perifornical area could mean that OX-R1 mediates the food intake-promoting effect of orexins. Detailed reports have shown a rich presence of orexin within all these nuclei.[3,10,21] Interestingly, hypocretin-1 injected into the LHA activates c-*fos* neuronal gene induction in the same nuclei, then resulting in Fos protein expression.[7,31] In addition, injection of orexin-A, but not orexin-B, in the paraventricular hypothalamic nucleus and perifornical area/LHA promotes feeding in rats.[9] As Trivedi *et al*.[51] have reported the presence of OX-R2 mRNA in some of these nuclei (paraventricular and ventromedial hypothalamic nuclei, LHA), the overall feeding effect of the peptides could be mediated through both receptors, OX-R1 and OX-R2. We are currently characterising the distribution of OX-R2-like immunoreactivity in the rat

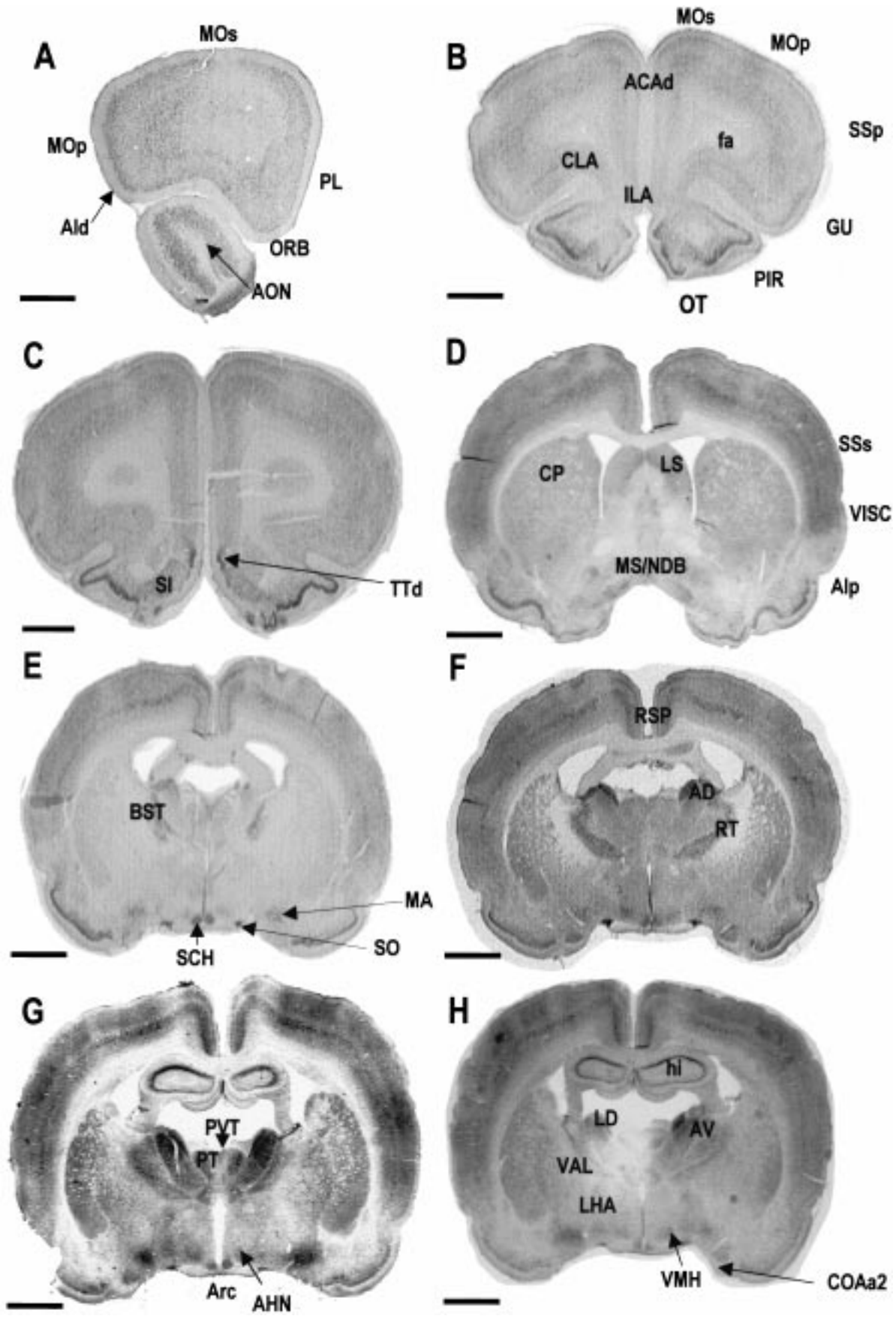
A
MOs
MOp
PL
AId
ORB
AON
B
MOs
MOp
ACAd
SSp
fa
CLA
ILA
GU
PIR
OT
C
SI
TTd
D
SSs
CP
LS
VISC
MS/NDB
AIp
E
BST
MA
SCH
SO
F
RSP
AD
RT
G
PVT
PT
Arc
AHN
H
hi
LD
AV
VAL
LHA
VMH
COAa2

Fig. 2.

brain to further investigate this question. The OX-R1-like immunosignals detected in the zona incerta, a region thought to regulate drinking behaviour, might be linked to the effect of orexins on water intake, as reported.[25] The strong immunosignal seen in the supraoptic nucleus might indicate that orexin, acting through OX-R1, regulates the antidiuretic vasopressin system.

The presence of hypothalamic OX-R1 in the arcuate and perifornical nuclei (the latter providing most of the excitatory synaptic input to paraventricular hypothalamic neurones for neuroendocrine control) could mediate neuroendocrine responses evoked upon injection of orexins. Studies have shown that i.c.v. injection of orexin-A causes a dose-dependent decrease in plasma growth hormone, thyroid-stimulating hormone and prolactin levels, while triggering a dose-dependent increase in corticosterone,[13,22,28] as well as modulating luteinising hormone release.[13,22,28] Application of orexins *in vitro* to hypothalamic slices containing the neuroendocrine cells at the arcuate nucleus level has an excitatory effect.[8,53] In addition, a predominant orexin-induced behaviour feature is grooming, closely associated with stress and feeding behaviours. The high density of OX-R1 immunoreactivity in both the supraoptic and paraventricular nuclei, where orexin injected i.c.v. induced Fos protein expression,[9] could suggest that the receptor mediates the effect of orexins on corticosterone release as reported,[13,22] possibly through the activation of corticotropin-releasing factor neurones, since OX-R1 is highly present within the parvicellular part of the paraventricular nucleus.

The presence of OX-R1-like immunoreactivity in the paraventricular thalamic nucleus, LHA and tuberomammillary hypothalamic nucleus, as well as in the preoptic area, pontine reticular formation, raphe nuclei, dorsal tegmental nuclei, vestibular nuclei and the locus coeruleus, is consistent with the arousal and hypnotic-related properties of orexins, as reported recently in rats[5,13,26] and in humans.[33] Since OX-R1 is present in the suprachiasmatic hypothalamic nucleus, it is possible that orexins are implicated in the circadian component of the sleep process as well. A recent report demonstrated that orexin-A modulated the sleep–wake cycle in rats,[38] and it has also been shown that orexin induced Fos protein expression in the suprachiasmatic hypothalamic nucleus.[9]

Strong OX-R1 immunoreactivity was found in the spinal cord and in the dorsal root ganglia, consistent with the detailed report of the robust innervation of the spinal cord by hypothalamic orexin-containing neurones and the activation of cultured rat spinal cord neurons to both orexins-A and -B.[52] As both the parvicellular part of the paraventricular hypothalamic nucleus and the LHA strongly project to the spinal cord (see Ref. 52) and strong OX-R1 immunostaining is present within these hypothalamic nuclei, there may be an OX-R1-responsive axis to provide a close association between the diencephalon and the spinal cord for feeding behaviour regulation.

The presence of OX-R1 in the spinal cord could suggest a widespread role for the orexins in regulating the parasympathetic and sympathetic activities of the autonomic nervous system. For instance, it has been reported that orexins increased heart rate and blood pressure in conscious rats.[7,40] More specifically, together with the presence of OX-R1 in several other CNS regions regulating pain (cingulate cortex, anterior thalamus and posterior hypothalamus, periaqueductal gray matter, trigeminal nucleus, dorsal root ganglia), it may be that orexins are important in nociception. Interestingly, van den Pol *et al.*[53] hypothesised that orexin neurones selectively innervated a C-fibre cell population (part of the system mediating pain-related sensory intense or noxious stimuli), and the present study has found that OX-R1 is localised on C-fibres.

In the cerebral and olfactory cortices, OX-R1-like immunostained cells were most likely principal pyramidal neurones. Discrete immunostained cells were found throughout the cortex, but were particularly noticeable in the infragranular layers. It may be that most of the cortical OX-R1 is not functional, since van den Pol *et al.*[53] reported that a small percentage (5%) of cultured rat cortical cells tested ($n = 122$) showed small electrical responses to orexin. The functional significance of the OX-R1 cortical immunostaining reported here is unknown, but this may be related to orexin control of feeding behaviour. Immunoreactivity was detected within the motor, sensory, visual, auditory and gustatory parts of the cortex, and signals were also found in metathalamic sensory relays such as the medial and lateral geniculate nuclei and their associated colliculi (the inferior and superior colliculi, respectively). A number of other structures regulating motor behaviour were OX-R1 immunopositive as well; amongst them there were some nuclei of the basal ganglia (neostriatum, globus pallidus, substantia nigra and subthalamic nucleus), some infracerebellar nuclei and nuclei belonging to the reticular formation, which localises central pattern generators such as in the trigeminal system (e.g. motor nucleus of the trigeminal nerve). The facial nerve nucleus was also labelled. Signals were also observed in

Fig. 2. Localisation of OX-R1 in a series of coronal rat brain sections, part I. OX-R1 was found throughout the isocortex: in the prelimbic and orbital areas (A), anterior cingulate part (B), motor regions (A, B), somatosensory parts (A, B), gustatory area (B), visceral and agranular insular areas (D), and the retrosplenial area (F). Many subcortical forebrain nuclei exhibited OX-R1-like immunoreactivity, such as the claustrum (B), the septal complex including the nucleus of the diagonal band, the lateral and medium septum (D), and the bed nucleus of the stria terminalis (E), the corpus striatum with immunostaining in the pallidum [i.e. substantia innominata (C), globus pallidus and magnocellular preoptic nucleus (E)] and the neostriatum (D). Olfactory regions were particularly rich in OX-R1 immunoreactivity, such as the olfactory nucleus (A), the olfacory tubercle and the piriform cortex (B, C). Amygdaloid regions showed immunoreactivity in the medial nucleus (H). Rostral diencephalon immunosignals were evident in the thalamus in the reticular nucleus (F), paraventricular, parataenial and anterodorsal nuclei (G), and the laterodorsal and anteroventral nuclei, as well as in the ventroposterior complex (H). Hypothalamic immunostained areas were the suprachiasmatic and supraoptic nuclei (E), arcuate nucleus (F), anterior nucleus (G), and the ventromedial and lateral nuclei (H). Scale bars = 200 μm.

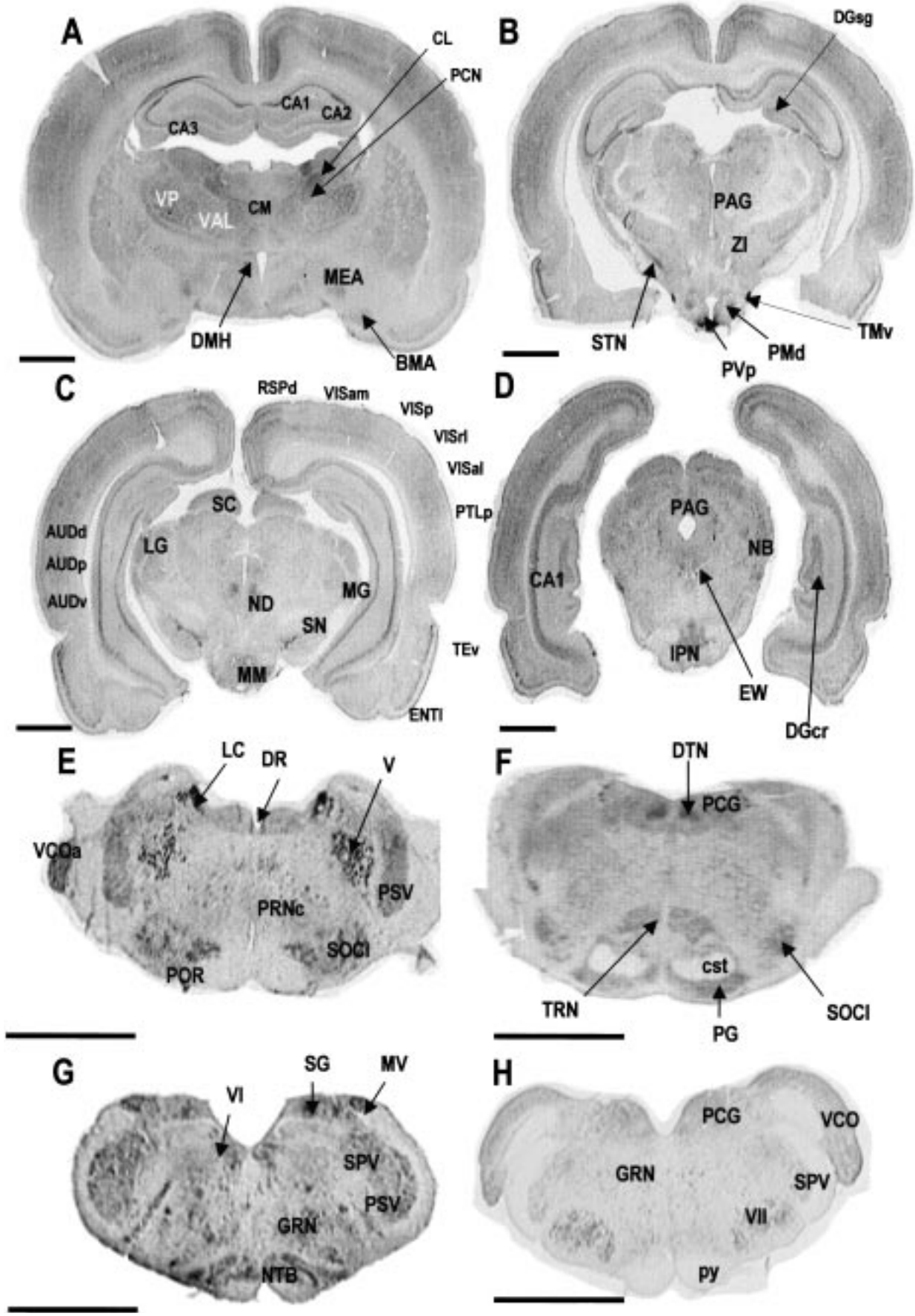
A
CL
PCN
CA1
CA2
CA3
VP
VAL
CM
MEA
DMH
BMA
B
DGsg
PAG
ZI
STN
PVp
PMd
TMv
C
RSPd
VISam
VISp
VISrl
VISal
PTLp
SC
AUDd
AUDp
AUDv
LG
MG
ND
SN
TEv
MM
ENTl
D
PAG
NB
CA1
IPN
EW
DGcr
E
LC
DR
V
VCOa
PSV
PRNc
SOCl
POR
F
DTN
PCG
cst
TRN
PG
SOCl
G
SG
MV
VI
SPV
PSV
GRN
NTB
H
PCG
VCO
GRN
SPV
VII
py

Fig. 3.

the lateral ventral thalamic nuclear subgroup, which receives a major input from the deep cerebellar nuclei. The thalamic nucleus is seen as a major relay station in the motor system linking the cerebellum, the basal ganglia and the cerebral cortex. Feeding behaviour is a complex activity which requires the activation of a large number of learning, memory, cognitive, emotional, somatosensorimotor and autonomic tasks related to the search for food and its processing (e.g. mastication).[27,30] It may be a function of orexins not only to control the energy balance through food intake, but also to modulate motor components of feeding behaviour, e.g. grooming.

Little immunoreactivity was found in the principal neurones of the hippocampal formation: the pyramidal cells of Ammon's horn were only faintly labelled. Interestingly, rat hippocampal neurones *in vitro* failed to elicit a response when challenged with orexins.[53] However, the hilus of the dentate gyrus contained OX-R1-immunoreactive interneurones.

Finally, we found evidence of OX-R1 within the amygdaloid nuclei and other forebrain limbic regions, such as the septum and the entorhinal cortex, traditionally referred to as control centres for emotion. Some nuclei in the thalamus also displayed high OX-R1 immunoreactivity. The anterodorsal and laterodorsal nuclei, also part of the limbic system, are known to establish reciprocal connections with the hypothalamic mammillary bodies, subserving regulation of emotion, while the mediodorsal nucleus is connected with the prefrontal cortex, a region known to modulate affection as well as integration of somatic visceral activities. Hence, it is probable that orexins regulate affect, as already proposed.[38] As discussed above, orexin regulates corticosterone release, and pathological hyperactivity of the stress axis is thought to contribute to the onset of depressive disorders.[24]

Comparison between the neuroanatomical distribution of the orexin-1 receptor protein and melanin-concentrating hormone receptor immunostaining in the rat CNS, and functional implications

MCH and orexins share many anatomical as well as physiological features. Both peptides are expressed in the zona incerta and LHA, constituting distinct and unique peptidergic markers of these regions (see Ref. 43). The LHA regulates many functions, probably because it projects widely throughout the nervous system (see Introduction). Consistent with this, MCH and orexin neurones project very widely thoughout the neuraxis.[2,37] Furthermore, there is much overlap between the projection sites of MCH and orexin processes, although a few differences are of interest, such as the autonomic preganglionic regions being richly innervated by orexin neurones[52] but not by MCH neurones.[2] Both peptides are orexigenic,[39,40] but while they share a common physiological end-point, both peptides can evoke opposite actions. For instance, while orexin-A induces intense grooming,[13] MCH has no effect on it *per se*, but will oppose α-melanocyte-stimulating hormone-induced grooming behaviour.[42] Previous work has shown that orexin and MCH hypothalamic neurones form separate cell populations.[3,10]

We very recently reported the distribution of the MCH receptor (SLC-1) in the rat CNS.[4,19] SLC-1 signals were observed in the cerebral cortex, caudate–putamen, hippocampal formation, amygdala, hypothalamus and thalamus, as well as in various nuclei of the mesencephalon and rhombencephalon. Regulation of feeding behaviour involves a plethora of peptides and neurotransmitters (for review, see Refs 11 and 29). For a further understanding of the interactions between these feeding regulators, which could ultimately lead to the treatment of feeding disorders, it will now be of interest to perform double localisation studies to determine whether a single neurone can express both types of receptor. Studies directed at MCH and orexin neurones, bearing one or the other or both receptors, are currently in progress.

Neither SLC-1 nor OX-R1 immunoreactivity has been detected in glial cells (as determined by morphological correlates and the absence of glial fibrillary acidic protein immunostaining in the SLC-1 and OX-R1 cells), which would indicate that MCH and orexin are not likely to play a direct role in brain immune regulation. While most of the immunolabelled neurones seen in the present study were pyramidal ones, interestingly, in the cerebral cortex, OX-R1 and MCH receptor cells, both preferentially present within layers III and IV, were mainly pyramidal neurones and interneurones, respectively. As for MCH (see Ref. 2), it may be that orexins also play a role in general arousal. There was a striking overlap between the SLC-1 and OX-R1 distributions in the hypothalamus. Immunostaining of both was present in the anterior

Fig. 3. Localisation of OX-R1 in a series of coronal rat brain sections, part II. OX-R1 was found in the visual areas and the auditory areas of the cortex (C). Amygdaloid regions showed immunoreactivity in the basomedial nucleus (A). Strong immunosignals were notable in the caudal thalamus, such as in the centrolateral, centromedian and paracentral nuclei (A), and metathalamic sensory processing regions such as the lateral and medial geniculate nuclei (C). Clear labelling was also seen in the subthalamic nucleus and zona incerta (B). Densely labelled regions in the hypothalamus were the dorsomedial nucleus (A) and mammillary regions such as the posterior (B) and the medial (C) nuclei, as well as the periventricular nucleus (B). The hippocampal formation exhibited OX-R1 immunoreactivity in the pyramidal layers of Ammon's horn (A), and in the granular (B) and crest (D) layers of the dentate gyrus. Hindbrain immunostaining was observed in the reticular core, such as in the central gray of the brain [nucleus of Darkschewitsch (C), periaqueductal gray matter (D), locus coeruleus (E), the dorsal tegmental nuclei and pontine central gray (F), and the supragenual nucleus (G)], the reticular formation [pontine (E), tegmental (F) and gigantocellular (G, H) reticular nuclei], the interpeduncular nucleus (D) and the raphe (dorsal nuclei in E). Other brainstem systems immunostained with the OX-R1 antiserum were the somatosensory system (principal trigeminal nucleus in E), the auditory system, such as the nucleus brachium of the inferior colliculus (D), the ventral cochlear nucleus and the superior olivary complex including the periolivary regions (E), and the nucleus of the trapezoid body (G). Labelling was also observed in vestibular nuclei such as the medial nucleus (G). Motor systems displayed OX-R1 immunoreactivity in the extrapyramidal system, such as the substantia nigra (C), the visceral Edinger–Westphal nucleus (D), the motor trigeminal nucleus (E), the abducens (G) and the facial (H) nuclei. Scale bars = 200 μm (A–D); 500 μm (E–H).

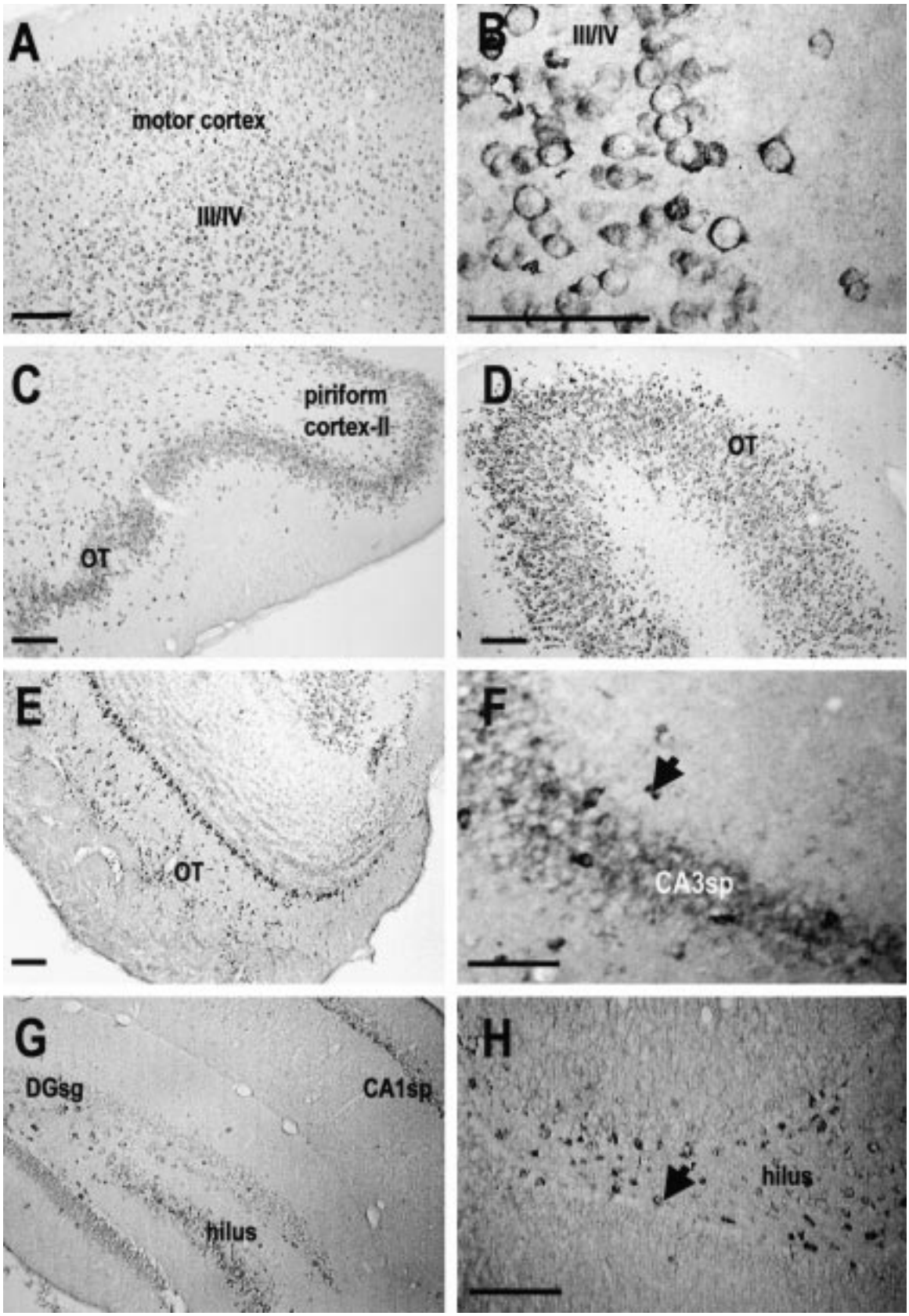

Fig. 4. OX-R1 immunoreactivity in the cortical areas and hippocampal formation of the rat brain. Numerous OX-R1 immunostained cells were detected throughout the isocortex, including the motor cortex (A). Immunostained cells were evident in layers III and IV (A, B). Note that the immunostained cells were labelled on the plasma membrane (B) as expected for the cell location of a G-protein-coupled receptor. Immunoreactivity was also abundant in olfactory regions, such as the olfactory tubercle (C–E) and the piriform cortex (C). OX-R1 immunosignals were also noticed in the hippocampal formation in the pyramidal cell layer of Ammon's horn (F, G) and the granular layer of the dentate gyrus (G, H), as well as in interneurones in the hilus (G, H). Scale bars = 500 μm.

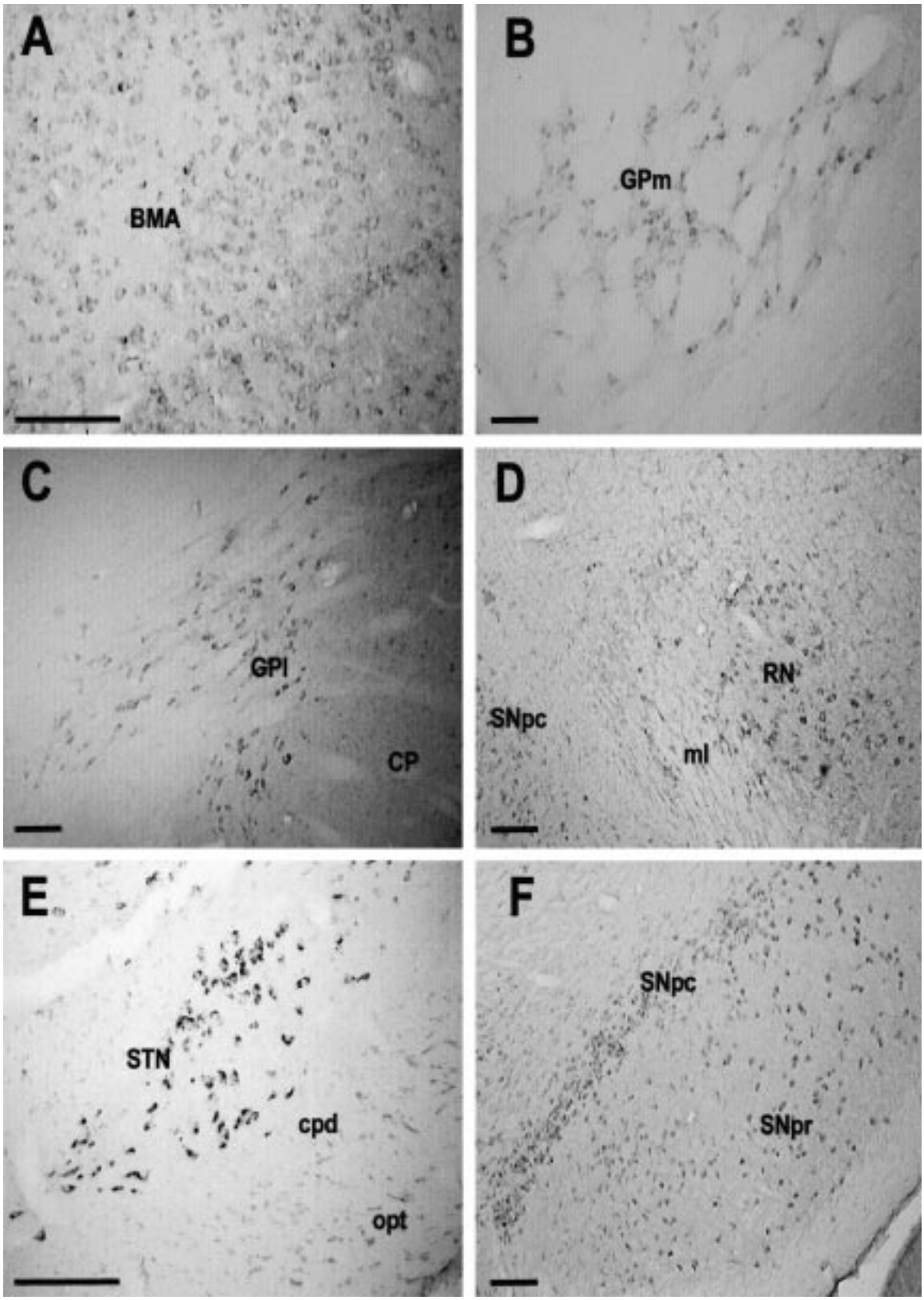

Fig. 5. OX-R1 immunoreactivity in the basal ganglia. Immunostaining was observed in the amygdaloid nuclei (such as the basomedial nucleus; A), the medial and lateral parts of the globus pallidus (B, C), the substantia nigra (pars compacta: D, F; pars reticulata: E, F) and the subthalamic nucleus (E). Scale bars = 500 μm.

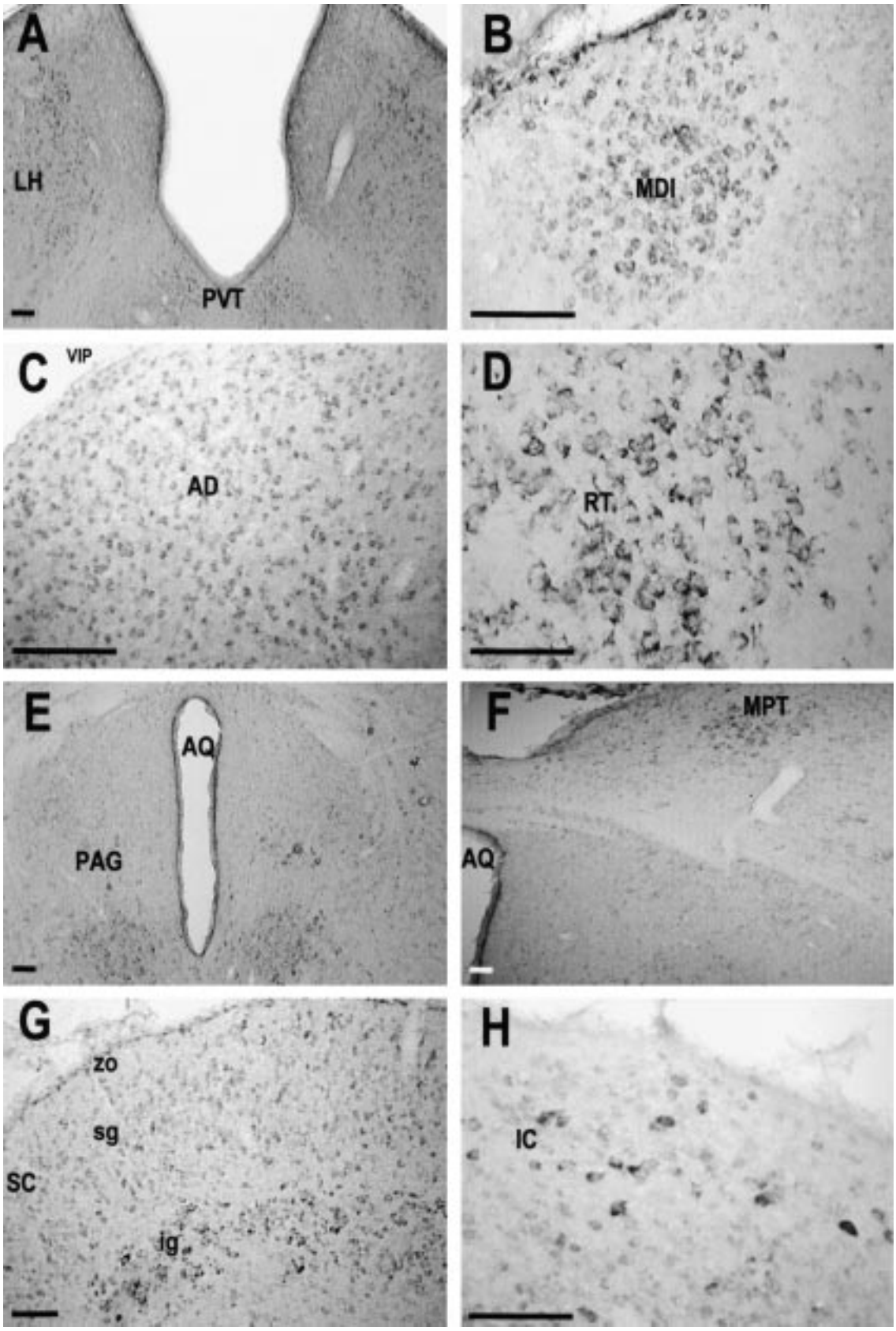

Fig. 6. OX-R1 immunoreactivity in the thalamus and epithalamus. Immunostaining for OX-R1 was detected in the lateral part of the habenula, as well in the paraventricular thalamus nucleus (A). Strong immunostaining was present in other thalamic nuclei, such as the mediodorsal thalamic nucleus (D), the anterodorsal thalamic nucleus (C) and the reticular nucleus (D). Light immunostaining was detected in the periaqueductal gray matter (E) and the medial pretectal area (F). In thalamic midbrain-associated regions, immunosignals were seen both in the superior colliculus (more particularly concentrated in the intermediate gray layer; G) and the inferior colliculus (H). Scale bars = 500 μm.

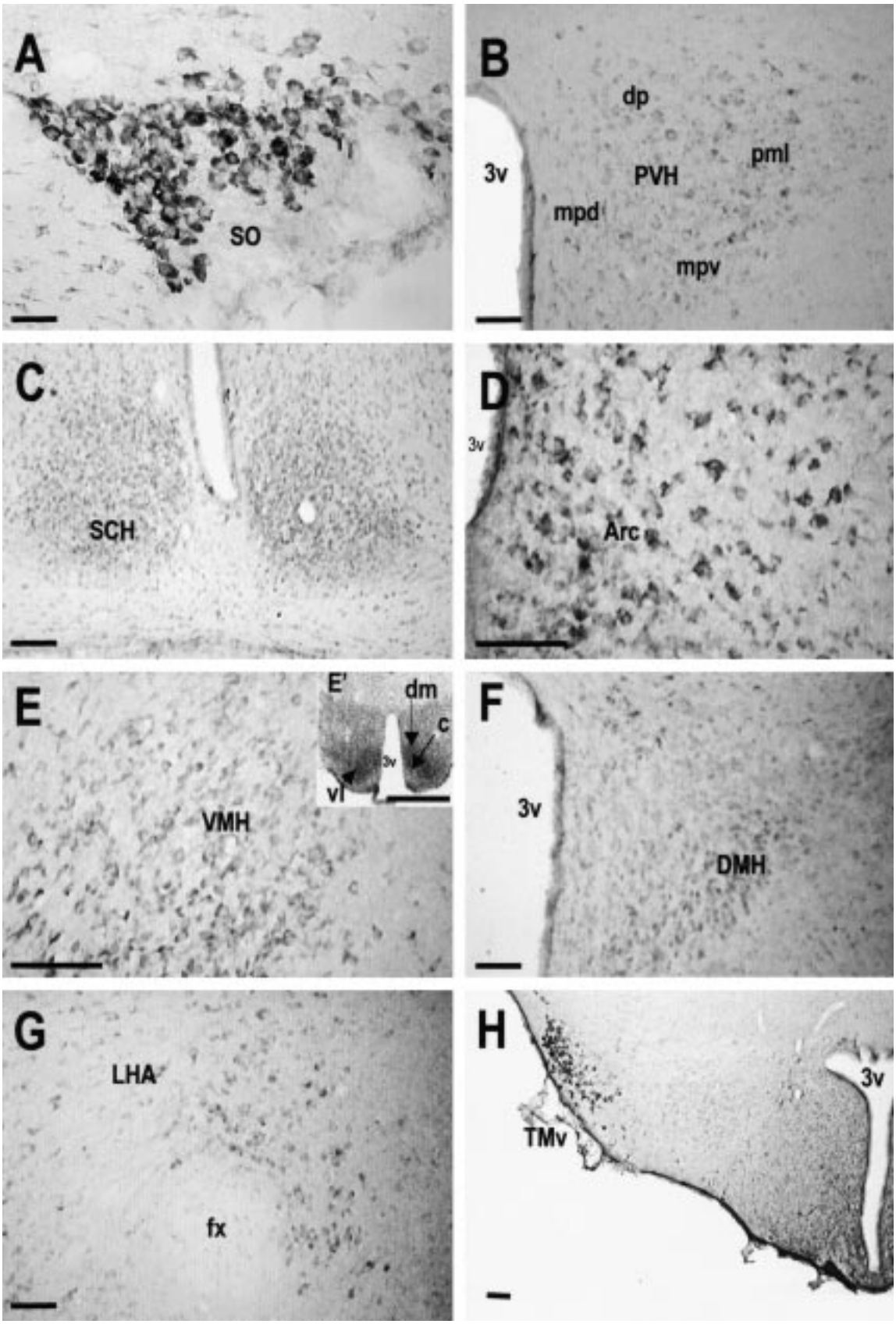

Fig. 7. OX-R1 immunoreactivity in the hypothalamus. A dense population of OX-R1-immunostained cells was detected in the supraoptic nucleus (A), paraventricular nucleus (B), suprachiasmatic nuclei (C), arcuate nucleus (D), ventromedial nucleus (E, E′), dorsomedial nucleus (F), perifornical area of the LHA (G) and the tuberomammillary nucleus (H). In the paraventricular nucleus, staining was present in the lateral zone of the posterior magnocellular region, dorsal parvicellular, medial parvicellular and the dorsal zone of the medial parvicellular region (B). In the ventromedial nucleus, all sub-regions were immunostained, i.e. the ventrolateral, dorsomedial and central parts (E′). Scale bars = 500 μm.

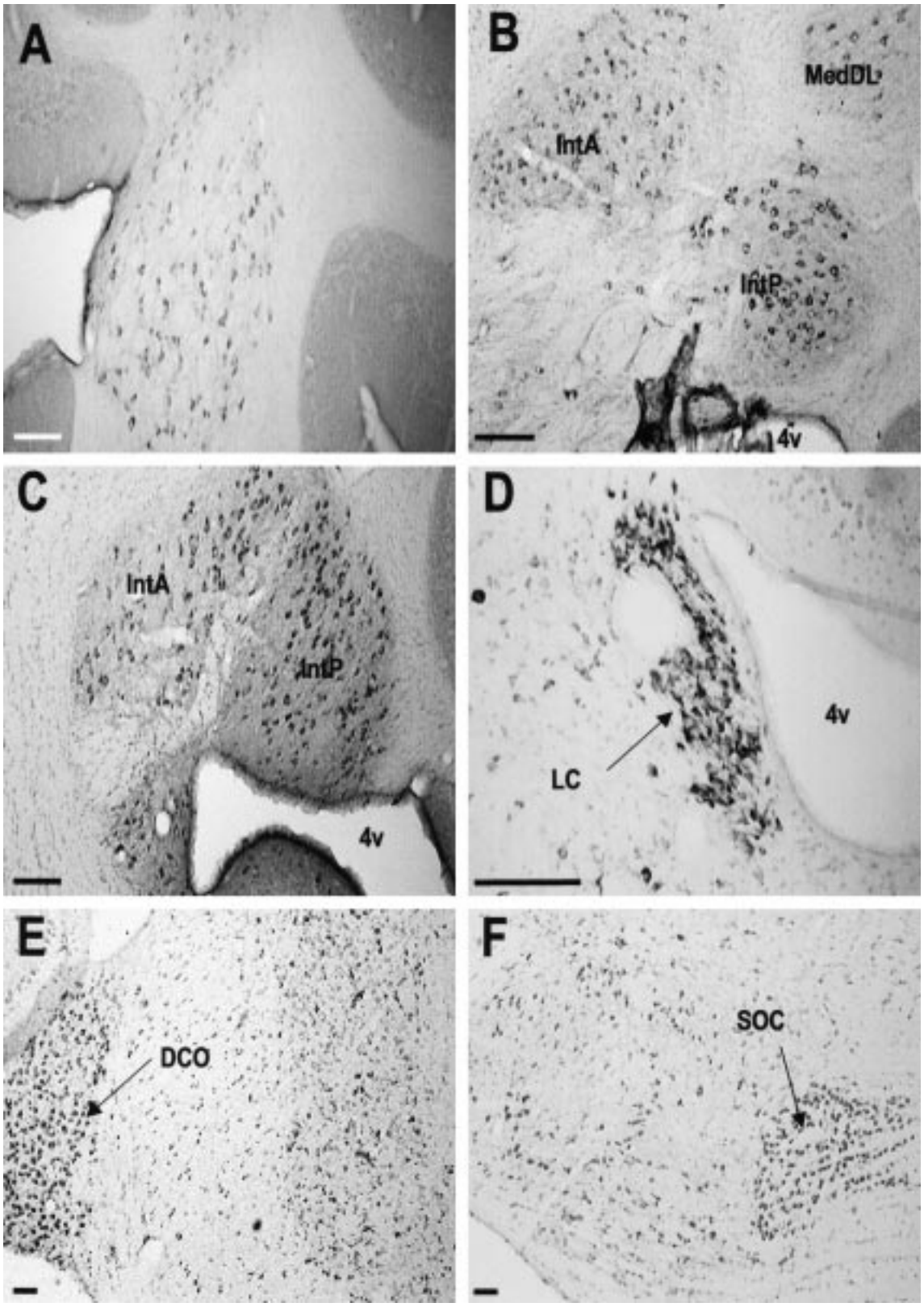

Fig. 8. OX-R1 immunoreactivity in the cerebellum and locus coeruleus. OX-R1 staining was detected in infracerebellar nuclei, such as the interpositi (B, C), as well as the medial nucleus (B). Strong OX-R1 immunosignals were observed in the locus coeruleus (D), the dorsal cochlear nucleus (E) and the superior olivary complex (F). Scale bars = 500 μm.

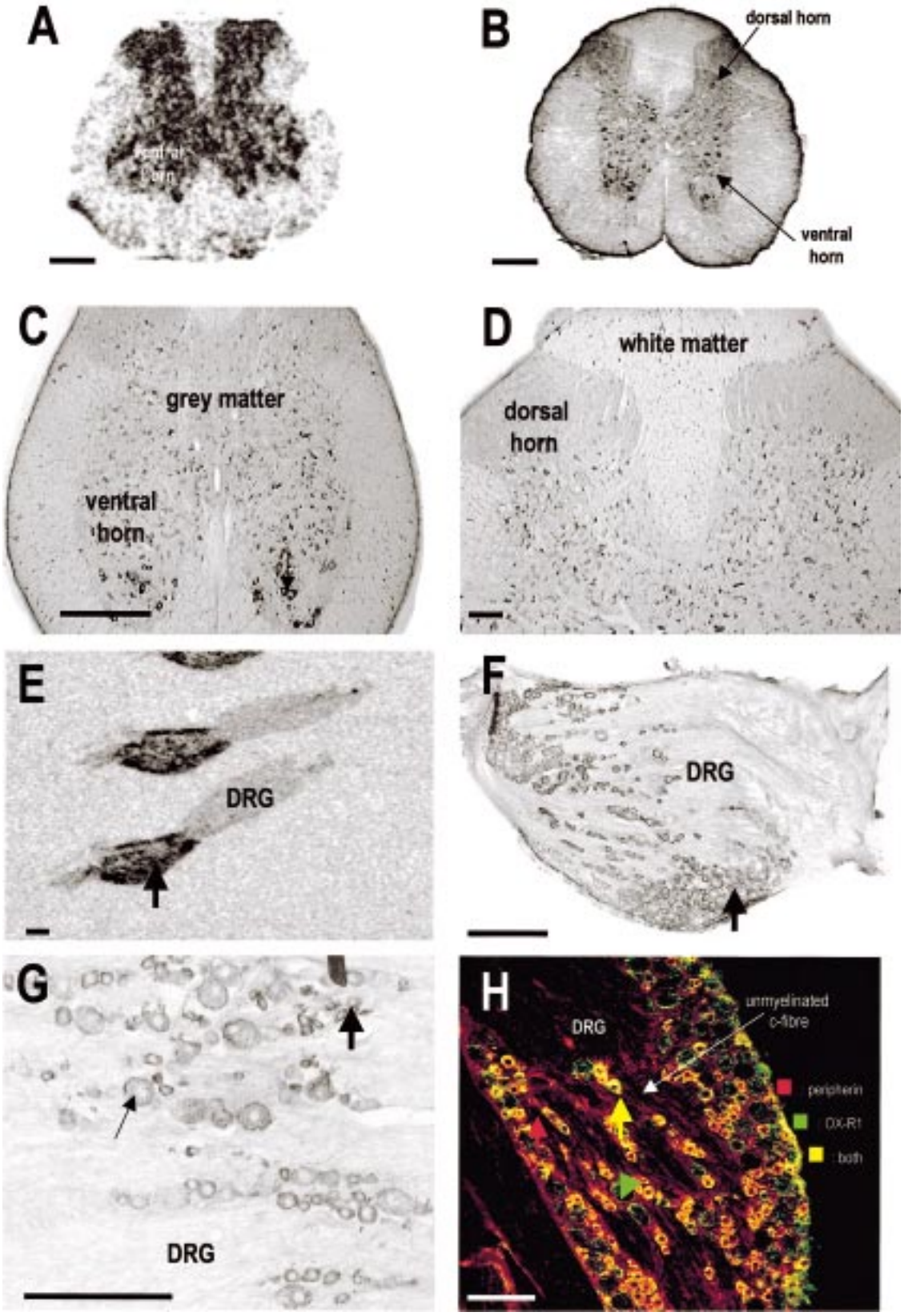

Fig. 9. OX-R1 immunoreactivity in the spinal cord and dorsal root ganglia. In the spinal cord, OX-R1 mRNA (A) and protein signals (B) were present within the gray matter of the spinal cord (note the overlap in A and B). Stained cells with the morphology of motoneurones were detected in the ventral horn (C). OX-R1 mRNA (A) and protein signals (B) were identified in the dorsal root ganglia (note the overlap in E and F). A higher magnification revealed two types of OX-R1-immunolabelled cells (G): large-diameter cells (thin arrow) and small-diameter cells (thick arrow). Co-localisation experiments revealed that some of the OX-R1 immunoreactivity associated with the small-diameter cells is co-expressed with peripherin, a marker of C fibres (yellow arrow), while OX-R1 large-diameter cells did not exhibit peripherin immunoreactivity (green arrowhead). A subset of the peripherin-immunopositive small cell population does not contain OX-R1 immunoreactivity (red arrow). Scale bars = 200 μm (A, B), 500 μm (C–H).

nucleus, magnocellular system (supraoptic and paraventricular nuclei), arcuate nucleus, dorso- and ventromedial nuclei, mammillary complex and tuberomammillary nucleus. Some differences in the sub-distribution could be found, however. In the paraventricular nucleus, it appeared that SLC-1 labelling was particularly dense in the magnocellular part, unlike OX-R1, which was distributed quite equally within the parvicellular and magnocellular parts. Many more OX-R1 cells were found in the LHA at the perifornical level than SLC-1 cells. Importantly, both receptors are also strongly expressed in the locus coeruleus, where orexin-A increases the neuronal electrical activity.[13] It may be that MCH also regulates the alertness, vigilance and arousal. Orexins could also play a major role in regulating electrolytic balance. Orexins affect drinking behaviour as much as angiotensin, and OX-R1 is present within brain osmolarity control centres (i.e. the supraoptic nuclei). Interestingly, orexins in the gut regulate secretomotor neurones.[23] This is similar to the properties of MCH in regulating electrolyte and water balance of the gastrointestinal tract.[17]

CONCLUSION

Using a selective antiserum raised against OX-R1, we have characterised the brain and spinal cord distribution of OX-R1 in the rat. Gene expression experiments (*in situ* hybridisation and quantitative RT–PCR) broadly confirmed our immunohistochemical findings: the receptor gene is expressed widely throughout the rat CNS, as also reported by others.[51] Our study would support the involvement of orexins in regulating feeding and drinking behaviours, neuroendocrine control and arousal, through the OX-R1 subtype at least. It is also predictive of a role for these peptides in the regulation of affect. OX-R1 is highly expressed in the limbic system and the locus coeruleus, both major structures regulating mood. Disruption of the feed-forward mechanism linking the corticotropin-releasing factor pathway between the hypothalamus and the locus coeruleus is throught to be involved in affective disorder. Orexin mimetics may prove to be useful psychotropics. It is likely that at least some of the biological actions of orexins are mediated through a co-operation of both receptor subtypes, OX-R1 and OX-R2. For instance, orexin-A binds equally to OX-R1 and OX-R2, and in the hypothalamus, both receptor subtypes are found in the same nuclei that regulate feeding behaviours. Preliminary results from this laboratory on the distribution of OX-R2 indicate a potential for overlap of both receptors on the same cell. Given that the *ox-r2* gene is not expressed in the locus coeruleus,[51] unlike OX-R1[51] (and this study), it would appear that OX-R1 is the receptor that is mainly involved in the control of arousal. It is a mutation in the *ox-r2* gene, however, that triggers narcolepsy. This is not inconsistent with many other neuropeptidergic systems; it is reminiscent of the orexigenic actions of neuropeptide Y, probably mediated via both neuropeptide Y-R1 and -R5 receptors, or the action of somatostatin on growth hormone release, controlled via both somatostatin receptor subtypes 1 and 2.[35]

REFERENCES

1. Bernardis L. L. and Bellinger L. L. (1996) The lateral hypothalamic area revisited: ingesting behavior. *Neurosci. Behav. Rev.* **20,** 189–287.
2. Bittencourt J. C., Press F., Arias C., Peto C., Vaughan J, Nahon J. L., Vale W. and Sawchenko P. E. (1992) The melanin-concentrating hormone system of the rat brain: an immuno- and hybridization histochemical characterisation. *J. comp. Neurol.* **319,** 218–245.
3. Broberger C., de Lecea L., Sutcliffe J. G. and Hokfelt T. (1998) Hypocretin/orexin- and melanin-concentrating hormone-expressing cells form distinct populations in the rodent lateral hypothalamus: relationship to the neuropeptide Y and agouti gene-related protein systems. *J. comp. Neurol.* **402,** 460–474.
4. Chambers J., Ames R. S., Bergsma D., Muir A., Fitzgerald L. R., Dytko G. M., Foley J. J., Martin J., Liu W. -S., Park J., Ellis C., Ganguly S., Konchar S., Cluderay J., Leslie R., Wilson S. and Sarau H. M. (1999) Melanin-concentrating hormone is the natural cognate ligand for the orphan G-protein coupled receptor SLC-1. *Nature* **400,** 261–265.
5. Chemelli R. M., Willie J. T., Sinton C. M., Elmquist J. K., Scammell T., Lee C., Richardson J. A., Williams S. C., Xiong Y., Kisanuki Y., Fitch T. E., Nakazato M., Hammer R. E., Saper C. B. and Yanagisawa M. (1999) Narcolepsy in orexin knockout mice: molecular genetics of sleep regulation. *Cell* **98,** 437–451.
6. Date Y., Mondal M. S., Matsukura S., Ueta Y., Yamashita H., Kaiya H., Kangawa K. and Nakazato M. (2000) Distribution of orexin/hypocretin in the rat median eminence and pituitary. *Molec. Brain Res.* **76,** 4–6.
7. Date Y., Ueta Y., Yamashita H., Yamaguchi H., Matsukura S., Kangawa K., Sakurai T., Yanagisawa M. and Nakazato M. (1999) Orexins, orexigenic hypothalamic peptides, interact with autonomic neuroendocrine and neuroregulatory systems. *Proc. natn. Acad. Sci. USA* **96,** 748–753.
8. Delecea L., Kilduff T. S., Peyrin C., Foye P. E., Danielson P. E., Fukuhara C., Battenberg E. L. F., Gautvik V. T., Bartlett F. S., Frankel W. N., van den Pol A. N., Bloom F. E., Gautvik K. M. and Sutcliffe J. G. (1998) The hypocretins: hypothalamus-specific peptides with neuroexcitatory activity. *Proc. natn. Acad. Sci. USA* **95,** 322–327.
9. Dube M. G., Kalra S. P. and Kalra P. S. (1999) Food intake elicited by central administration of orexins/hypocretins: identification of hyothalamic sites of action. *Brain Res.* **842,** 437–477.
10. Elias C. F., Saper C. B., Eleftheria M.-F., Tritos N. A., Lee C., Kelly J., Tatro J. B., Hoffman G. E., Ollmann M. M., Barsh G. S., Sakurai T., Yanagisawa M. and Elmquist J. K. (1998) Chemically defined projections linking the mediobasal hypothalamus and the lateral hypothalamic area. *J. comp. Neurol.* **402,** 442–459.
11. Flier J. S. and Maratos-Flier E. (1998) Obesity and the hypothalamus: novel peptides for new pathways. *Cell* **92,** 437–440.
12. Grillon S., Herve C., Griffond B. and Fellmann D. (1997) Exploring the expression of the melanin-concentrating hormone messenger RNA in the rat lateral hypothalamus after gold–thioglucose injection. *Neuropeptides* **31,** 131–136.
13. Hagan J. J., Leslie R. A., Patel S., Evans M. L., Wattam T. A., Holmes S., Benham C. D., Taylor S. G., Routledge C., Hemmati P., Munton R. P., Ashmeade T. E., Shah A. S., Hatcher J. P., Hatcher P. D., Jones D. N. C., Smith M. I., Piper D. C., Hunter A. J., Porter R. A. and Upton N. (1999) Orexin-A activates locus coeruleus cell firing and increases arousal in the rat. *Proc. natn. Acad. Sci. USA* **96,** 10,911–10,916.
14. Harrison D. C., Medhurst A. D., Bond B. C., Campbell C. A., Davis R. P. and Philpott K. L. (2000) The use of quantitative RT–PCR to measure mRNA expression in a rat model of focal ischemia—caspase-3 as a case study. *Molec. Brain Res.* **75,** 143–149.

15. Haynes A. C., Jackson B., Overend P., Buckingham R. E., Wilson S., Tadayyon M. and Arch J. R. S. (1999) Effects of single and chronic intracerebroventricular administration of theorexins on feeding in the rat. *Peptides* **20,** 1099–1105.
16. Hervieu G. and Nahon J. L. (1995) Pro-melanin-concentrating hormone messenger ribonucleic acid and peptides expression in peripheral tissues of the rat. *Neuroendocrinology* **61,** 348–364.
17. Hervieu G., Volant K., Grishina O., Descroix-Vagne M. and Nahon J. L. (1995) Similarities in cellular expression and functions of melanin-concentrating hormone and atrial natriuretic factor in the rat digestive tract. *Endocrinology* **137,** 561–571.
18. Hervieu G. and Emson P. C. (1998) The localisation of somatostatin receptor 1 sst_1 immunoreactivity in the rat brain using an N-terminal specific antibody. *Neuroscience* **85,** 1263–1284.
19. Hervieu G. J., Cluderay J. E., Harrison D., Meakin J., Maycox P., Nasir S. and Leslie R. A. (2000) The distribution of the mRNA and protein products of the melanin-concentrating hormone (MCH) receptor gene, slc-1, in the central nervous system of the rat. *Eur. J. Neurosci.* **12,** 1194–1216.
20. Hervieu G. J., Cluderay J. E. and Leslie R. A. (2000) The distribution of the OX-R1 protein in the rat brain. *Eur. J. Neurosci.* **12,** (Suppl. 11) 182.1.
21. Horvath T. L., Diano S. and van den Pol A. N. (1999) Synaptic interaction between hypocretin (orexin) and neuropeptide Y cells in the rodent and primate hypothalamus: a novel circuit implicated in metabolic and endocrine regulations. *J. Neurosci.* **19,** 1072–1087.
22. Ida T., Nakahara K., Murakami T., Hanada R., Nakazato M. and Murakami N. (2000) Possible involvement of orexin in the stress reaction in rats. *Biochem. biophys. Res. Commun.* **270,** 318–323.
23. Kirchgessner A. L. and Liu M.-T. (1999) Orexin synthesis and response in the gut. *Neuron* **24,** 941–951.
24. Koob G. F. (1999) Corticotropin-releasing factor, norepinephrine, and stress. *Biol. Psychiat.* **46,** 1167–1180.
25. Kunii K., Yamanaka A., Nambu T., Matsuzaki I., Goto K. and Sakurai T. (1999) Orexins/hypocretins regulate drinking behaviour. *Brain Res.* **842,** 256–261.
26. Lin L., Faraco J., Li R., Kadotani H., Rogers W., Lin X., Qiu X., de Jong P. J., Nishino S. and Mignot E. (1999) The sleep disorder canine narcolepsy is caused by a mutation in the hypocretin (orexin) receptor 2 gene. *Cell* **98,** 365–376.
27. Lund J. P., Kolta A., Westberg K. -G. and Scott G. (1999) Brainstem mechanisms underlying feeding behaviors. *Curr. Opin. Neurobiol.* **8,** 718–724.
28. Mitsuma T., Hirroka Y., Kayama M., Adachi K., Rhue N., Ping J. and Nogimori T. (1999) Effects of orexin-A on TRH and TSH secretion in rats. *Horm. Metab. Res.* **31,** 606–609.
29. Moriguchi T., Sakurai T., Nambu T., Yanagisawa M. and Goto K. (1999) Neurons containing orexin in the lateral hypothalamic area of the adult rat brain are activated by insulin-induced acute hypoglycemia. *Neurosci. Lett.* **264,** 101–104.
30. Morley J. E. (1987) Neuropeptide regulation of appetite and weight. *Endocr. Rev.* **8,** 256–287.
31. Mullett M. A., Billington C. J., Levine A. S. and Kotz C. M. (2000) Hypocretin I in the lateral hypothalamus activates key feeding-regulatory brain sites. *NeuroReport* **11,** 103–108.
32. Nambu T., Sakurai T., Mizukami K, Hosoya Y., Yanagisawa M. and Goto M. (1999) Distribution of orexin neurons in the adult rat brain. *Brain Res.* **827,** 243–260.
33. Nishino S., Ripley B., Overeem S., Lammers G. J. and Mignot E. (2000) Hypocretin (orexin) deficiency in human narcolepsy. *Lancet* **355,** (9197) 39–41.
34. Ostrander E. A. and Giniger E. (1999) Let sleeping dogs lie? *Nature Genet.* **23,** 3–4.
35. Patel Y. C. and Srikant C. B. (1998) Somatostatin receptors. *Trends Endocr. Metab.* **8,** 398–405.
36. Paxinos G. and Watson C. (1998) The Rat Brain in Stereotaxic Coordinates, 3rd edn, Academic, San Diego.
37. Peyron C., Tighe D. K., van den Pol A. N., de Lecea L., Heller H. C., Sutcliffe J. G. and Kilduff T. S. (1998) Neurons containing hypocretin (orexin) project to multiple neuronal systems. *J. Neurosci.* **18,** 9996–10,015.
38. Piper D. C., Upton N., Smith M. I. and Hunter A. J. (2000) The novel brain neuropeptide, orexin-A, modulates the sleep–wake cycle of rats. *Eur. J. Neurosci.* **12,** 726–730.
39. Qu D., Ludwig D. S., Gammeltoft S., Piper M., Pelleymounter M. A., Cullen M. J., Mathes W. F., Przypek J., Kanarek R. and Maratos-Flier E. (1996) A role for melanin-concentrating hormone in the central regulation of feeding behaviour. *Nature* **380,** 243–244.
40. Sakurai T., Amemiya A., Ishii M., Matsuzaki I., Chemelli R. M., Tanaka H., Williams S. C., Richardson J. A., Kozlowski G. P., Wilson S., Arch J. R. S., Buckingham R. E., Haynes A. C., Carr S. A., Annan R. S., McNulty D. E., Liu W. -S., Terret J. A., Elshourbagy N. A., Bergsma D. J. and Yanagisawa M. (1998) Orexins and orexin receptors: a family of hypothalamic neuropeptides and G-protein-coupled receptors that regulate feeding behavior. *Cell* **92,** 573–585.
41. Samson W. K., Gosnell B., Chang J. -K., Resch Z. T. and Murphy T. C. (1999) Cardiovascular regulatory actions of the hypocretins in the brain. *Brain Res.* **831,** 248–253.
42. Sanchez M., Baker I. and Celis M. (1997) Melanin-concentrating hormone (MCH) antagonizes the effects of α-MSH and neuropeptide E-I on grooming and locomotor activities in the rat. *Peptides* **18,** 393–396.
43. Sawchenko P. E. (1998) Toward a new neurobiology of energy balance, appetite and obesity. The anatomists weigh-in. *J. comp. Neurol.* **402,** 435–441.
44. Siegel J. M (1999) Narcolepsy: a key role for hypocretins (Orexins). *Cell* **98,** 409–412.
45. Smart D., Jerman J. C., Brough S. J., Neville W. A., Jewitt F. and Porter R. A. (2000) The hypocretins are weak agonists at recombinant human orexin-1 and orexin-2 receptors. *Br. J. Pharmac.* **129,** 1289–1291.
46. Smart D., Jerman J. C., Brough S. J., Rushton S. L., Murdock P. R., Jewitt F., Elshourbagy N. A., Ellis C. E., Middlemiss D. N. and Brown F. (1999) Characterization of recombinant human orexin receptor pharmacology in a Chinese hamster ovary cell-line using FLIPR. *Br. J. Pharmac.* **128,** 1–3.
47. Swanson L. W. (1992) Brain Maps: Structure of the Rat Brain, Elsevier, Amsterdam.
48. Taheri S., Mahmoodi M., Opaka-Juffry J., Ghater M. A. and Bloom S. R. (1999) Distribution and quantification of immunoreactive orexin A in rat tissues. *Fedn Eur. biochem. Socs Lett.* **457,** 157–161.
49. Taheri S., Ward H., Ghatei M. and Bloom S. (2000) Role of orexins in sleep and arousal mechanisms. *Lancet* **355,** (9206) 847.
50. Takahashi J. S. (1999) Narcolepsy genes wake up the sleep field. *Science* **285,** 2076.
51. Trivedi P., Yu H., Douglas J., MacNeil L. H. T., der Ploeg V. and Guan X. -M. (1998) Distribution of orexin receptor mRNA in the rat brain. *Fedn Eur. biochem. Socs Lett.* **438,** 71–75.
52. van den Pol A. N. (1999) Hypothalamic hypocretin (orexin): robust innervation of the spinal cord. *J. Neurosci.* **19,** 3171–3182.
53. van den Pol A., Gao X. -B., Obrietan K., Kilduff T. S. and Belousov A. B. (2000) Presynaptic and postsynaptic actions and modulation of neuroendocrine neurons by a new hypothalamic peptide, hypocretin/orexin. *J. Neurosci.* **18,** 7962–7970.

(*Accepted* 12 *January* 2001)